A Microwave Analog of a Quantum Double Well Potential

A thesis submitted in partial fulfillment of the requirement
for the degree of Bachelor of Science with Honors in
Physics from the College of William and Mary in Virginia,

by

Salvatore Guenther Yonan Rego

Accepted for _____
(Honors or no-Honors)

_____
Advisor: Professor Seth Aubin

_____
Prof. Len Neighbors

_____
Prof. Keith Griffioen

Williamsburg, Virginia
May 4, 2023

Contents

Acknowledgments **iii**

List of Figures **vii**

List of Tables **viii**

Abstract **v**

1 Introduction **1**

1.1 Scientific Motivation 1

1.2 Engineering and Pedagogical Motivations 2

1.3 Structure of Thesis 3

2 Twin Microstrip Physics **4**

2.1 Quantum Analog 4

3 Simulating Microstrip Systems **11**

3.1 Learning Software 11

3.2 Sonnet Single Trace Tests 12

3.3 Sonnet Curved Trace Tests 13

3.4 FEKO Straight Trace Tests 14

3.5 FEKO Curved Trace Tests 15

3.6 Twin Microstrip System 18
3.7 Twin Microstrip System Final Board Design 23

4 Experimental Apparatus **25**
4.1 Fabrication of a Microwave Transmission Pickup Coil 25
4.2 Data Collection With Microwave Transmission Pickup Coil 28
4.3 Physical Apparatus of Twin Microstrip System 31

5 Results **34**
5.1 7 GHz Data 34
5.2 14 GHz Data 38

6 Conclusion/Outlook **44**

A Fabrication of Microwave Transmission Pickup Coil **46**

B Code sample **50**

C Making Curves in Eagle **51**

Acknowledgments

Many people support this work, and it would have been impossible to achieve this work without help and support. I am incredibly thankful and lucky to have the support of my parents, John Rego and Roxane Yonan as well as my siblings, Atticus Rego and Alexandra Rego who have supported me every step of the way. I would like to thank my research advisor Dr. Seth Aubin for suggesting this project to me and for his continuous guidance throughout my time at William Mary. I would also like to thank the other lab members William Miyahira, Cate Sturner, and Jordan Shields. Finally, I would like to acknowledge all of the friends who have helped me along the way, especially Sydney Greco, Adi de la Guardia, and Javier Chiriboga all of whom went above and beyond to support me. I have not always expressed it verbally, but I truly appreciate the help I received from everyone more than they could ever imagine.

List of Figures

1.1 An image of the FEKO simulation where we can see the current hopping back and forth between the two traces. Each arrow shows a hop of the current from one trace to the other. Green represents a region of high current density, while blue represents an area of low current density. 2

2.1 $|A\rangle$, The left image shows a superposition of the other two wavefunctions, the groundstate configuration in the middle, $|g\rangle$, and the 1st odd excited state $|e\rangle$. 5

2.2 Images of the microwave current at a given moment in time in the twin microstrip system. The left image shows all of the microwave current being within the left trace as a superposition of the other two images. The right image shows the current traveling in both traces perfectly in phase ($\phi = 0$), while the middle image shows the current traveling 180 degrees out of phase($\phi = 180$). 6

2.3 This image depicts a plot of the probability, $P_A(t)$, of finding the particle in Well A vs. Time. 9

3.1 An image of a Sonnet simulation model with both ends of the trace curved. This model uses the Rogers 4350B substrate, with 0.017 mm thick and 3.7 mm wide copper traces. The board is 1.524 mm thick and 10 cm long by 3.5cm wide, and the curves have a turn radius of 37 mm. 14

3.2 An image of the FEKO simulation. Here, the triangles represent the mesh that the program creates before it runs the simulation. This simulation uses RO4350B substrate, 0.017 mm thick and 1.5 mm wide copper traces. The board is 1.524 mm thick, and 10 cm long by 5 cm wide. 15

3.3 An image of the early FEKO simulation with a single sharp curve. This model uses the RO4350B substrate. The board is 1.5 mm thick and 10 cm long by 4.5 cm wide, 3.7 mm wide copper traces. The radius of the curve is 6 mm. 17

3.4 An image of a FEKO simulation with both ends of the trace curved. The board substrate is RO4350B and 1.524 mm thick. The traces are 3.7 mm wide, and the curve radius is 35.65 mm. 18

3.5 FEKO current simulation demonstrating the current "hopping" effect. The current is seen as the highlighted green portion of the trace. Frequency = 9 GHz. The board has a total length of L = 100 cm. 19

3.6 A plot of $\frac{\lambda_{hop}}{2}$ vs. the Frequency in GHz compiled from Sonnet simulations. 20

3.7 Sonnet 9 GHz current simulation results. The length of the board is L = 50 cm. 21

3.8 FEKO 9 GHz current simulation results.The length of the board is L = 50 cm. 21

3.9 A plot of the number of hops vs. frequency created using data from Sonnet simulations. 22
3.10 Image of the board design in Eagle. Board Specs: trace width = 3.7 mm, PCB Board = RO4350B, board thickness - 1.524 mm = 0.06", turn radius = 35.65 mm 23

4.1 An image of the pickup coil placed next to a ruler for scale. 26
4.2 A close up image of the loop at the end of the pickup coil. 27
4.3 Picture of the experimental setup, for measuring a standing wave along a single copper trace. 29
4.4 Plot of Voltage vs. Distance along trace depicting the shape of a standing wave, at 7 GHz. The standing wave is supported by a 50 Ω microstrip transmission line on a RO4350B microwave PCB board (thickness = 1.524 mm = 0.06") with a trace width of 3.7 mm. 30
4.5 An image showing the twin microstrip system apparatus. The microwaves enter the setup on the trace 1 input. 32
4.6 Experimental setup for measuring the hopping back-and-forth effect in the twin microstrip system. 33

5.1 A plot of Voltage vs. Distance at the 7 GHz frequency. The microwaves are injected on Trace 1 on the position x=0 side. 35
5.2 A plot of the running average of Voltage vs. Distance at the 7GHz frequency. 36
5.3 A plot of the running average of Voltage vs. Distance at the 7 GHz frequency overlaid with the actual data for Trace 2. 37

5.4 An image showing the current mapping for a Sonnet simulation of the twin microstrip system running at 7 GHz. This simulation predicts $\lambda_{hop} = 40$ cm. 38
5.5 A plot of Voltage vs. Distance at the 14 GHz frequency. The microwaves are inserted on trace 1 on the x=0 position side. 39
5.6 A plot of the running average of Pickup Coil Voltage vs. Distance at the 14 GHz frequency. This plot indicates $\lambda_{hop} = 28$ cm or $\lambda_{hop} = 15$ cm. 40
5.7 A plot of the running average of Pickup Coil Voltage vs. Distance at the 14 GHz frequency overlaid with the actual data for Trace 1. . . . 40
5.8 An image showing the current mapping for a Sonnet simulation of the twin microstrip system running at 12 GHz. 41
5.9 An image showing the current mapping for a Sonnet simulation of the twin microstrip system running at 14 GHz. This simulation predicts $\lambda_{hop} = 30$ cm. 41
5.10 An image showing the current mapping for a Sonnet simulation of the twin microstrip system running at 14.5 GHz. 42

A.1 Exposed teflon layer after the removal of the copper layer. 47
A.2 The loop formed from the inner conductor layer. 48
A.3 Completed loop soldered together. 49

C.1 An image showing the eagle display. 52

List of Tables

2.1 This table provides a summary of analogous quantities between the quantum double well system and the microwave twin microstrip system. I is the microwave current. $\vec{B}$ is the microwave magnetic near field, and $\vec{E}$ is the microwave electric near field. 10

Abstract

The objective of this project is the observation and measurement of the back-and-forth hopping of microwave current between two parallel microstrip transmission lines. The effect of current "hopping" was observed first in simulation, and then in experiment by injecting a microwave current into a single microstrip transmission line next to a second parallel one. After simulating the effect with two different software applications, a prototyping circuit board (PCB) was designed and constructed to study it experimentally. In order to run tests with the PCB board, a pickup coil was constructed to enable measurements of the microwave magnetic near field, which serves as a proxy for the microwave current in a microstrip trace. With the new apparatus, tests were conducted at 7 GHz and 14 GHz. The 14 GHz test showed that current hopped from one trace to the other and back. This effect is the microwave analog of a particle in a quantum double well potential.

Chapter 1

Introduction

1.1 Scientific Motivation

The scientific motivation for this project is both to better understand the coupling between two microstrip transmission lines (see Fig. 1.1), and how the microwave near field is modified by this coupling. In particular, the effect of the coupling on the transverse and axial profiles of the microwave near field and its polarization components is very important for designing AC Zeeman traps based on parallel microstrips [1]. The AC proximity effect, related to the AC skin effect, is fairly sensitive to the phase of the currents in neighboring microstrips [1]. It can also contribute significantly to the resulting near field. This thesis presents the design, simulation, construction, and testing of a twin microstrip test apparatus. This apparatus enables the investigation of this behavior experimentally. This apparatus can also be used to test computed near fields based on commercial microwave simulation software. Finally, the twin microstrip setup is a stepping stone to a triple microstrip scheme, which is a key design element for microwave AC Zeeman trapping [1].

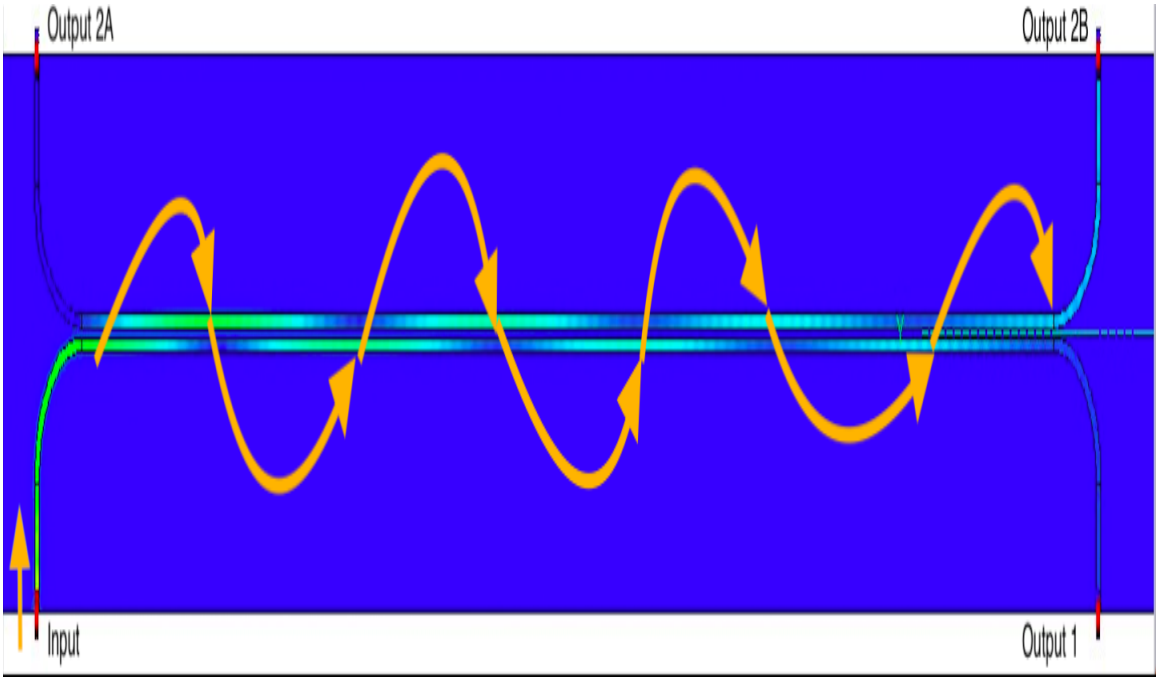

Figure 1.1: An image of the FEKO simulation where we can see the current hopping back and forth between the two traces. Each arrow shows a hop of the current from one trace to the other. Green represents a region of high current density, while blue represents an area of low current density.

Examining Figure 1.1, when a microwave current is injected into a single trace, it does not do what we might expect classically. Instead of staying within the trace and traveling to the end, it instead will jump back and forth between the two traces, indicated by the arrows. This image shows a simulation of the current hopping effect that we will later see experimentally.

1.2 Engineering and Pedagogical Motivations

Engineers are aware of this effect and some of its potential uses. Indeed, this effect can be leveraged to make a "beam splitter" for microwave currents. By altering the length of the two traces, we can control the amount of microwave current that will "hop" from one trace to the other. Perhaps we desire 90% of the current

in the left trace, or maybe 50%-50% is better suited for that particular application. While electrical engineers have a good understanding of how to use this effect to get a desired amount of power to the required location, they are less concerned with the specific distribution and shape of the magnetic and electric fields as they propagate throughout the system. A deeper understanding of these quantities would greatly benefit the design of microwave atom chips and other devices with parallel microstrip transmission lines.

Pedagogically, the twin microstrip apparatus is well suited as a classroom demonstration of quantum double-well physics using a microwave analog. While the phenomenological physics of the back and forth hopping of the current is straightforward, it is also fairly unintuitive, and it is a good illustration of the importance of describing waves in terms of eigenmodes. Such a demonstration could be useful for both quantum mechanics and electrodynamics courses.

1.3 Structure of Thesis

This thesis is structured in the following manner: Chapter 2 presents the theory of the quantum double well potential and how it relates to the twin microstrip system. Chapter 3 provides information on the software simulations of twin microstrip systems and some of the different design iterations that I went through. Chapter 4 details the process of data collection and also describes the experimental setup. Chapter 5 presents the results of two sets of data collection. Finally, chapter 6 provides my conclusions as well as a future outlook for the project.

Chapter 2

Twin Microstrip Physics

This chapter discusses the physics behind the twin microstrip system by using a particle in a quantum double well potential as an analog for the system. It covers the general idea of how the "hopping back and forth" effect works, as well as how we can solve this system mathematically.

2.1 Quantum Analog

The hopping back-and-forth effect is due to the wave nature of the microwaves, and as such the physics could manifest itself in a quantum system with matter waves. The quantum analog of this system is a double well potential. Since this is an "even" potential (with respect to the center of it), we must consider both the even and odd modes of the wavefunction. As shown in Fig. 2.1, the ground state of this system is even, since it will have an equal probability amplitude of being in either of the two minima. The first excited state however will have its probability amplitude in one of the two wells inverted so it can be seen as an odd function. So, when we look at a superposition of the two; if they add together the probability will be concentrated in one of the two wells, however if they subtract then the converse will occur.

Likewise, having all of the microwave current/power/field on the right microstrip trace can be seen as an equal sum of the odd and even microwave propagation eigen-

modes (see Fig. 2.2). The particle will "hop" from one well to the other because the odd eigenstate evolves faster in time (i.e. travels faster) than the even one, and so the sum becomes a subtraction, so we now would have constructive interference in the left well and destructive interference in the right well. In the following figures, the bottom leftmost configuration is a sum of the two following it.

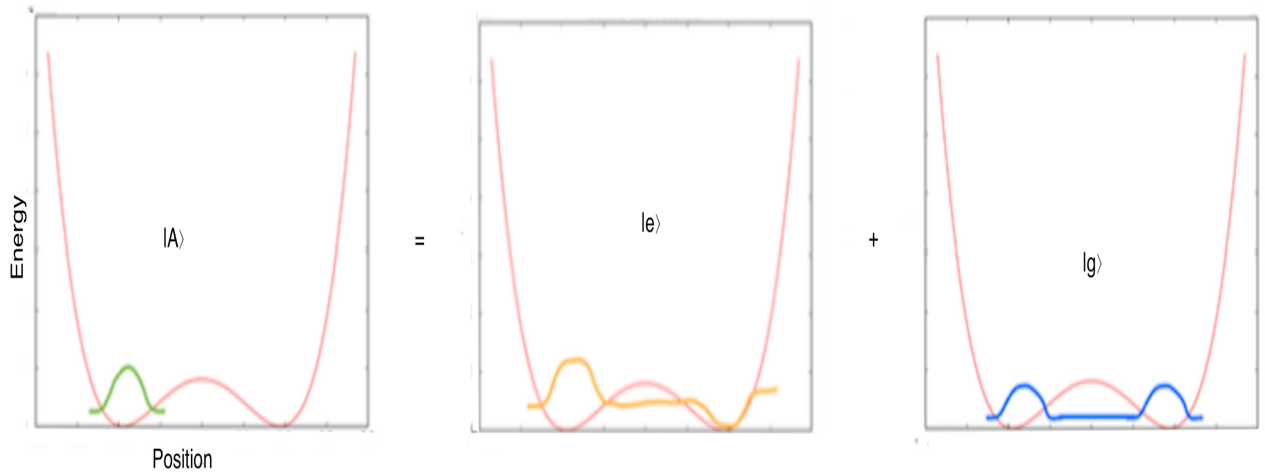

Figure 2.1: $|A\rangle$, The left image shows a superposition of the other two wavefunctions, the groundstate configuration in the middle, $|g\rangle$, and the 1st odd excited state $|e\rangle$.

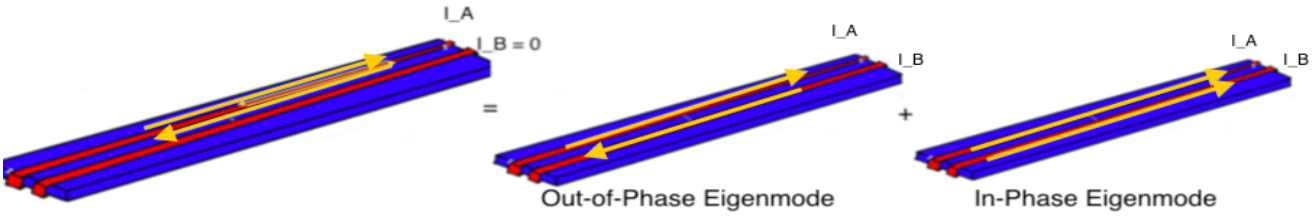

Figure 2.2: Images of the microwave current at a given moment in time in the twin microstrip system. The left image shows all of the microwave current being within the left trace as a superposition of the other two images. The right image shows the current traveling in both traces perfectly in phase ($\phi = 0$), while the middle image shows the current traveling 180 degrees out of phase($\phi = 180$).

Mathematical Formulation

The quantum double well can be understood qualitatively in the following manner. There are two eigenstates of this potential, the ground state and the first excited state. We can represent the ground eigenstate, $|g\rangle$, of the system as a superposition of states $|A\rangle$ and $|B\rangle$, i.e. a particle in well A, $|A\rangle$, or a particle in well B, $|B\rangle$. The first excited eigenstate, $|e\rangle$, is another linear combination of states A and B, however they are subtracted this time.

$$\begin{aligned} |g\rangle &= |A\rangle + |B\rangle \\ |e\rangle &= |A\rangle - |B\rangle \end{aligned} \tag{2.1}$$

Because these two states are eigenstates of the system, investigating the time evolution of $|g\rangle$ and $|e\rangle$ is straightforward. For the ground state $|g\rangle$ we have the corresponding energy, E_g, and for the first excited state $|e\rangle$ we will use E_e.

$$
\begin{aligned}
|g(t)\rangle &= e^{-i\frac{E_g}{\hbar}t}\,|g\rangle \\
|e(t)\rangle &= e^{-i\frac{E_e}{\hbar}t}\,|e\rangle
\end{aligned}
\tag{2.2}
$$

Now that we have established these two states, we can investigate the behavior in either of the two wells. In the case of a particle exclusively in well A, i.e. $|A\rangle$ state, both the ground state and first excited state have a positive amplitude. So, we can get our wavefunction for A by adding the two.

$$
\begin{aligned}
|g\rangle + |e\rangle &= 2\,|A\rangle \\
\frac{\alpha}{2}(|g\rangle + |e\rangle) &= |A\rangle
\end{aligned}
\tag{2.3}
$$

Where α allows us to normalize the state:

$$
\begin{aligned}
|A|^2 = \langle A|A\rangle = \frac{\alpha^2}{4}(\langle g| + \langle e|)(|g\rangle + |e\rangle) &= 1 \\
\frac{\alpha^2}{4}(\langle g|g\rangle + \langle g|e\rangle + \langle e|g\rangle + \langle e|e\rangle) &= 1 \\
\frac{\alpha^2}{4}(1+0+0+1) &= 1 \\
\frac{\alpha^2}{2} &= 1 \\
\alpha^2 &= 2 \\
\alpha &= \sqrt{2} \\
|A\rangle &= \frac{1}{\sqrt{2}}(|g\rangle + |e\rangle)
\end{aligned}
\tag{2.4}
$$

It is also straightforward to solve for state B, since we simply must subtract the two eigenstates from each other. We can see that the normalization constant here is the same.

$$|B\rangle = \frac{1}{\sqrt{2}}(\langle g| - \langle e|) \tag{2.5}$$

Considering the time evolution of state A, we have:

$$|A(t)\rangle = \frac{1}{\sqrt{2}}(|g(t)\rangle + |e(t)\rangle) = \frac{1}{\sqrt{2}}(e^{-i\frac{E_g}{\hbar}t}\,|g\rangle + e^{-i\frac{E_e}{\hbar}t}\,|e\rangle) \tag{2.6}$$

Now that we have established the time evolving description of the wavefunction for a particle initially in well A, we can consider the probability, $P_A(t)$, of the particle being found in that well at a later time:

$$\begin{aligned} P_A = |\,\langle A|A(t)\rangle\,|^2 &= |\frac{1}{2}(\langle g| + \langle e|)(e^{-i\frac{E_g}{\hbar}t}\,|g\rangle + e^{-i\frac{E_e}{\hbar}t}\,|e\rangle)|^2 \\ P_A = |\frac{1}{4}(e^{-i\frac{E_g}{\hbar}t} + e^{-i\frac{E_e}{\hbar}t})|^2 &= \frac{1}{4}|e^{-i\frac{E_g}{\hbar}t}(1 + e^{-i\frac{E_e - E_g}{\hbar}t})|^2 \\ P_A = \frac{1}{4}|1 + e^{-i\Delta\omega t}|^2 &= \frac{1}{4}|e^{-i\frac{\Delta\omega}{2}t}(e^{i\frac{\Delta\omega}{2}t} + e^{-i\frac{\Delta\omega}{2}t})|^2 \\ P_A = |\frac{e^{i\frac{\Delta\omega}{2}t} + e^{-i\frac{\Delta\omega}{2}t}}{2}|^2 &= |\cos\frac{\Delta\omega}{2}t|^2 = \cos^2\frac{\Delta\omega}{2}t \end{aligned} \tag{2.7}$$

Here, we simplified our expression with two substitutions. First, we take $\frac{E_g - E_e}{\hbar}$ and replace it with $\frac{\Delta E}{\hbar}$. We then replace $\frac{\Delta E}{\hbar}$ once more with $\Delta\omega$. Also, we must use Euler's Formula, $\frac{e^{ix}+e^{-ix}}{2} = cos(x)$ to substitute in and obtain our final expression, $P_A(t) = \cos^2\frac{\Delta\omega}{2}t$. By plotting this function, we obtain the time evolution of $P_A(t)$ shown in Fig. 2.3

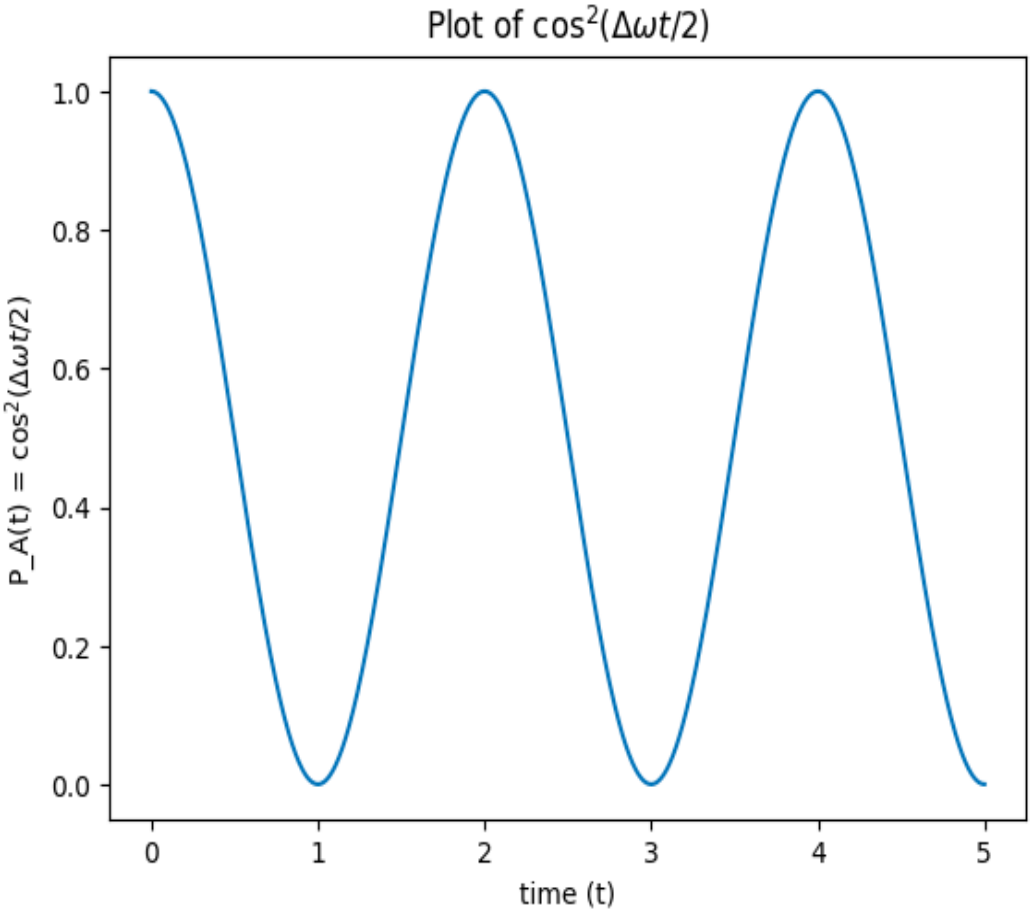

Figure 2.3: This image depicts a plot of the probability, $P_A(t)$, of finding the particle in Well A vs. Time.

The plot in Fig. 2.3 is interesting, because in this system we can clearly see the periodic nature of the particle existing in Well A, and then tunneling over to Well B, and then returning to well A, and so on.

In the quantum double-well system, the particle being in $|A\rangle$ corresponds to the microwave current being in Trace A. Likewise, the energy E of an eigenstate corresponds to the velocity v of the microwave eigenmode propagating down the twin microstrip system. Table 2.1 gives the analogous quantities in the two system.

Quantum Double-Well	Microwave Twin Microstrip System
$\langle x\|A\rangle$	$I_A, \overrightarrow{B_A}, \overrightarrow{E_A}$
E_g	v_{even}
$\langle x\|B\rangle$	$I_B, \overrightarrow{B_B}, \overrightarrow{E_B}$
E_e	v_{odd}
time	axial position
ΔE	Δv

Table 2.1: This table provides a summary of analogous quantities between the quantum double well system and the microwave twin microstrip system. I is the microwave current. $\vec{B}$ is the microwave magnetic near field, and $\vec{E}$ is the microwave electric near field.

Chapter 3

Simulating Microstrip Systems

The first milestone of this research project was to simulate the twin microstrip system. I used two different simulation software programs this semester: Sonnet and FEKO. While I used these two different programs to simulate similar systems, they are very different. FEKO is notably more complex than Sonnet but often yields more detailed results in the long run, albeit taking notably longer to run. Sonnet, on the other hand, is simple to use and the simulations run extremely quickly. Both are useful, and Professor Aubin suggested using Sonnet to "get one's foot in the door," then using FEKO to flush things out in greater detail. The three most important quantities we will gain from these simulations are the mapping of the currents (and thus observing the hopping back-and-forth effect), calculating the reflection coefficient, and calculating the impedance. In order to begin this milestone, I first had to learn how to operate the two software.

3.1 Learning Software

Per Professor Aubin's recommendation, I focused on learning Sonnet for my initial simulations, due to its $2D$ modeling approach, which I found very easy to follow. I began by watching and following along with two different tutorials to create basic and easy-to-understand systems. Although these two simulations did not contribute any

meaningful results or data to my research project, they helped me understand the basics of using Sonnet, and I felt confident to start simulating more relevant systems. The most crucial piece of information I learned about Sonnet during this time was how it dealt with curves. Sonnet divides the specified box into several cells defined by the users' size. However, during the simulation, Sonnet rounds out all of the numbers to fit within a cell. Therefore, if I have a cell length of 0.1 mm, and I try to make a shape with a length of 0.12 mm, Sonnet will round down and cram it into a single cell. This information would be very important later when I began simulating curved systems.

Several weeks later, I embarked on a similar learning process to become familiar with using FEKO. I quickly discovered that FEKO had rather different layout than Sonnet. It provides the user with a 3D model representation and generally produces more information about the microwave fields. Initially, I followed a step-by-step YouTube video to recreate a simple design. Once finished, I attempted a slightly more challenging task of simulating one of Professor Aubin's microstrip designs to see if I could obtain similar results. This proved to be more difficult, but after some time, I successfully completed the task and advanced from level 0. Unlike Sonnet, FEKO has no difficulty creating curves and simulating them.

3.2 Sonnet Single Trace Tests

After learning the Sonnet software, I conducted several simulations of simple single microstrip systems over a period of about two weeks. These simulations yielded consistent results, and served to deepen my understanding of the software and our goals: minimizing the reflection coefficient while attempting to keep the impedance around 50 Ω. During this time, I also discovered that the total number of cells directly affects the simulation time. For the straight trace tests, this was not an issue

as the rectangular shapes fit neatly into the cells, resulting in quick simulations. The reflection coefficients for these tests were acceptably small, ranging from about 0.1 to 0.001. Following these tests, I began exploring curved traces.

3.3 Sonnet Curved Trace Tests

The reason it became important for me to add curves to my simulations is because the final design will require the traces to be curved in order to have all of the necessary components fit on the board. So, I set out to learn how to make curves in Sonnet. Sonnet makes it incredibly simple to do this. The system I found easiest was when I used the tool that allowed the user to make a donut shape. I found that if I used this tool and specified the inner and outer radii so that the difference between the two was the width of the trace, then I would create a donut shape of the desired size. If I then specified the start and end angle of the shape being created, then I would end up with an arc with a constant width throughout (and thus constant impedance).

After figuring this out, I made two more simulations of a trace with a 90° curve. The first simulation had broken everything up into components: an initial horizontal trace, a 90° turn, and the final trace segment. While these were all touching each other, I had concerns that since they were different components, it might affect the simulation negatively. In order to test my concerns, I made a replica of my initial curved trace simulation except this time instead of creating an arc from the donut tool, I traced out the exact shape of it using the polygon trace tool, and succeeded in making the entire component system into a single unified component. After running this simulation and comparing it to my initial results, I found that they were identical and that I had unfortunately wasted my time. However, I now know that I no longer have to worry about having numerous different piecewise components for a trace since it will not affect the results of the simulations. This information will expedite any

future Sonnet simulations I do. Unfortunately, after these two simulations, we lost the license for the Sonnet software. While we have thankfully regained it, these were the last Sonnet simulations I did for some time. One such simulation model can be seen in Fig. 3.1

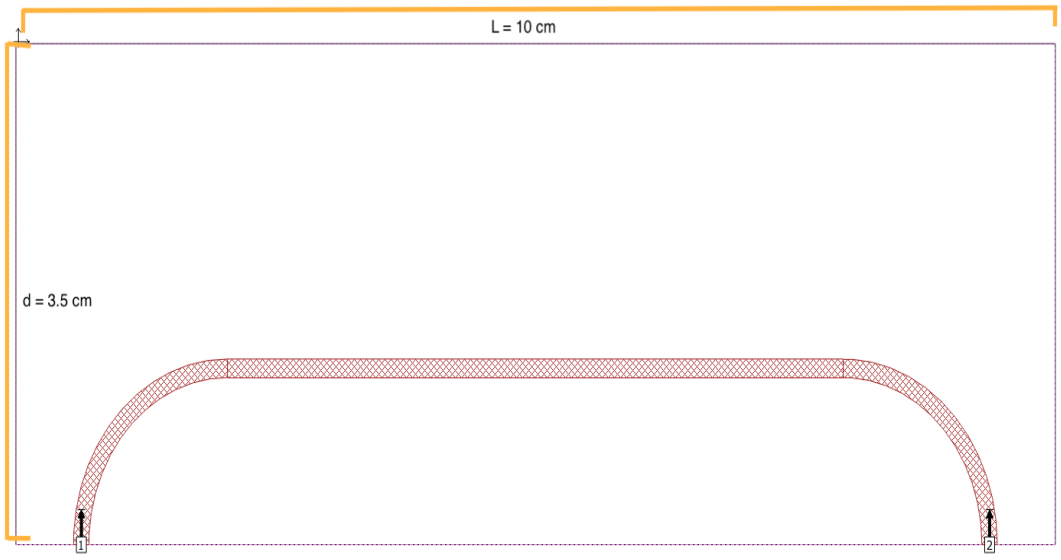

Figure 3.1: An image of a Sonnet simulation model with both ends of the trace curved. This model uses the Rogers 4350B substrate, with 0.017 mm thick and 3.7 mm wide copper traces. The board is 1.524 mm thick and 10 cm long by 3.5cm wide, and the curves have a turn radius of 37 mm.

3.4 FEKO Straight Trace Tests

After transitioning to FEKO and successfully completing the preliminary tests, I proceeded to simulate straight traces. In total, I ran two simulations of these basic systems, systematically varying almost every parameter, with the most critical being the substrate material. For my first test, I used an aluminum nitride substrate as seen in Fig. 3.2, but for the second, I switched to the Rogers RO4350B substrate, which is what we will use for the actual experiment. I discovered that aluminum

nitride performed slightly better than Rogers at minimizing the reflection coefficient and impedance. These two simulations aided in my continued acclimation to the software.

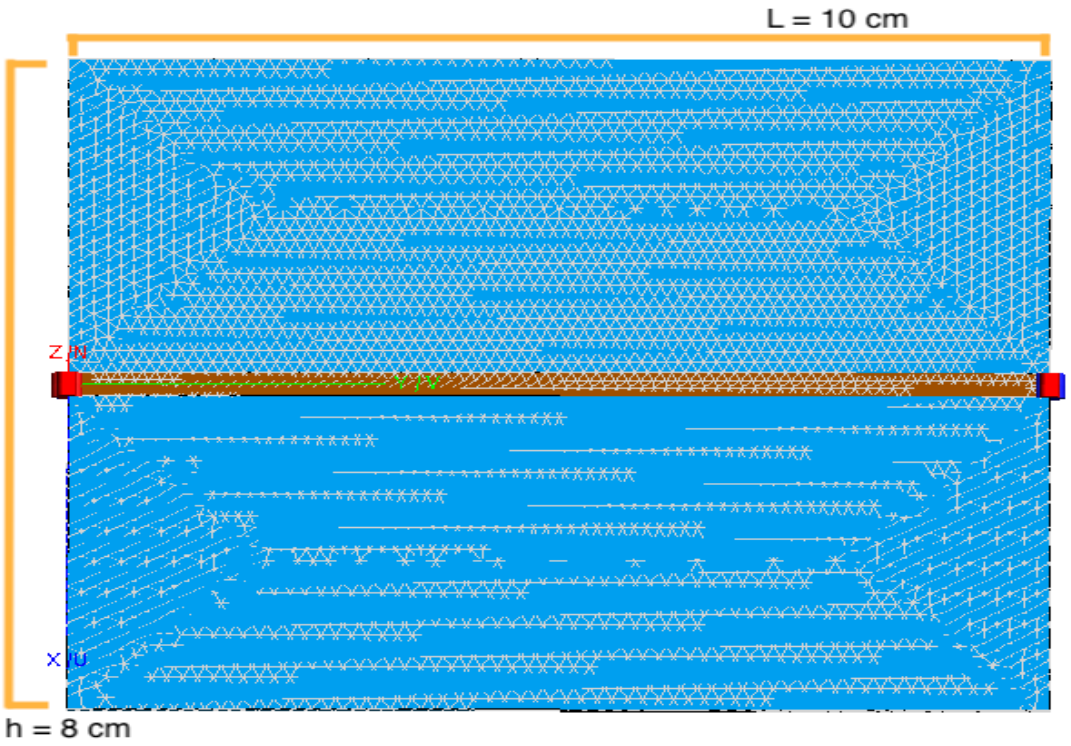

Figure 3.2: An image of the FEKO simulation. Here, the triangles represent the mesh that the program creates before it runs the simulation. This simulation uses RO4350B substrate, 0.017 mm thick and 1.5 mm wide copper traces. The board is 1.524 mm thick, and 10 cm long by 5 cm wide.

3.5 FEKO Curved Trace Tests

The computer modeling became more interesting when I started simulating single curved traces using FEKO. Fortunately, Shuangli Du's Ph.D thesis [2] provided all the necessary documentation on how to create curves within FEKO, and after following the instructions, I made several curved traces. The first trace I created was as simple as my designs for Sonnet. However, upon examining the current mapping in

this design, I found that a significant amount of current had accumulated within the inside edge of the curve. This was problematic because ideally, for a single trace, we would like the current to be nearly uniform throughout the trace. After discussing this with Professor Aubin, I learned that it is crucial to ensure that the radius of the curve is substantially larger than the width of the trace when constructing a curved trace; otherwise, issues such as the one I observed would occur. Fig. 3.3 shows a FEKO model with a problematic curve radius.

My second and third simulations took the need for a larger turn radius into account. Upon constructing a trace where the radius of the curve was 10 times larger than the width of the trace, I found no irregularities when examining the current mapping. For my third simulation, I used the specifications provided by Professor Aubin's 2022 summer simulations using a substrate of RO4350B: $\epsilon_r = 3.48 \tan\delta = 0.0037$, board thickness = 1.524 mm, trace width = 3.7 mm. These are the same numbers that are used when constructing the physical experiment, so I solely used these specifications from this point onward. Fig. 3.4 shows one of the FEKO double curve simulations with the corrected curve radius.

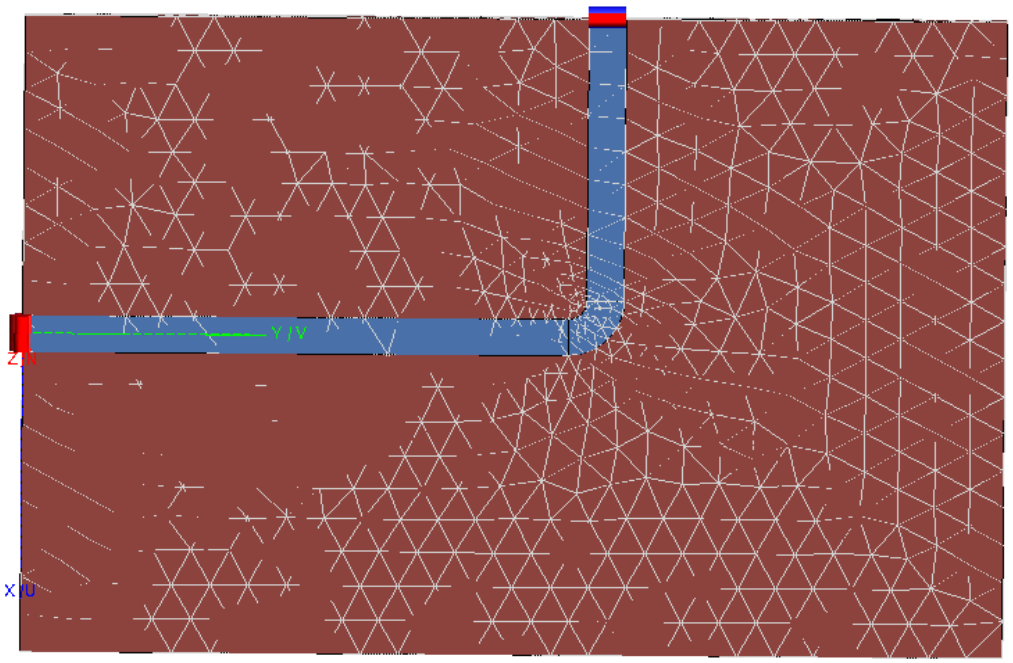

Figure 3.3: An image of the early FEKO simulation with a single sharp curve. This model uses the RO4350B substrate. The board is 1.5 mm thick and 10 cm long by 4.5 cm wide, 3.7 mm wide copper traces. The radius of the curve is 6 mm.

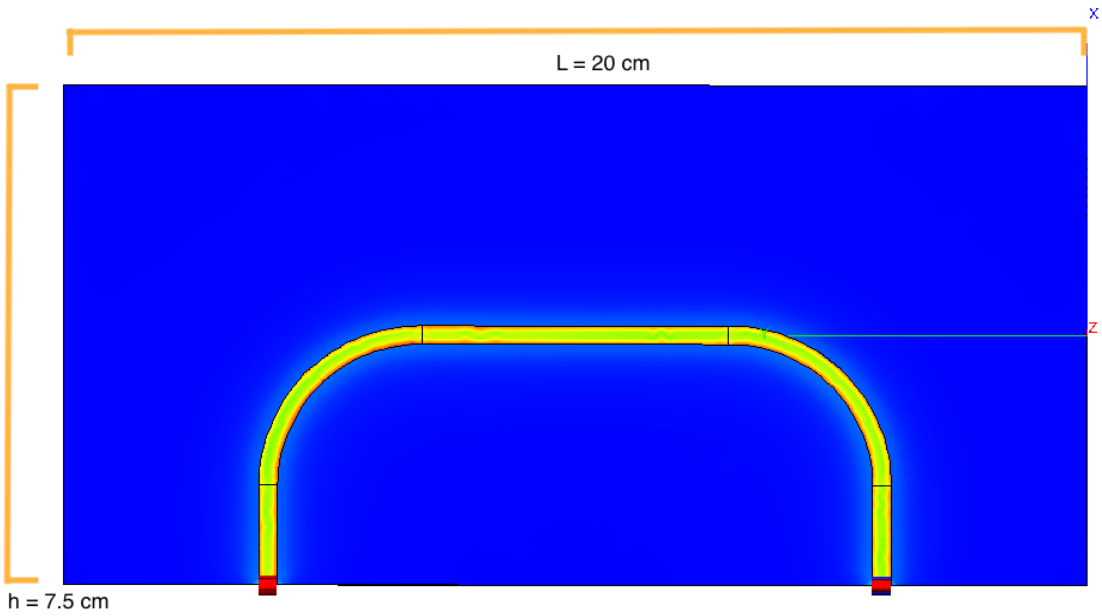

Figure 3.4: An image of a FEKO simulation with both ends of the trace curved. The board substrate is RO4350B and 1.524 mm thick. The traces are 3.7 mm wide, and the curve radius is 35.65 mm.

3.6 Twin Microstrip System

After achieving promising results in simulations of curved traces using both FEKO and Sonnet, I proceeded to design and construct the twin microstrip system. The microstrips were curved on both ends to provide SMA connectors for the circulators. I explored several design options but eventually settled on a larger design that would sufficiently demonstrate the effect. However, due to a mistake in unit conversions, the board ended up being over a meter in length. Although this proved problematic when ordering the physical board, it was a simple enough mistake to correct, and the large simulations provided useful data.

After conducting multiple simulations, I determined that the crucial quantity to focus on is the distance between the two traces. They must be close enough to al-

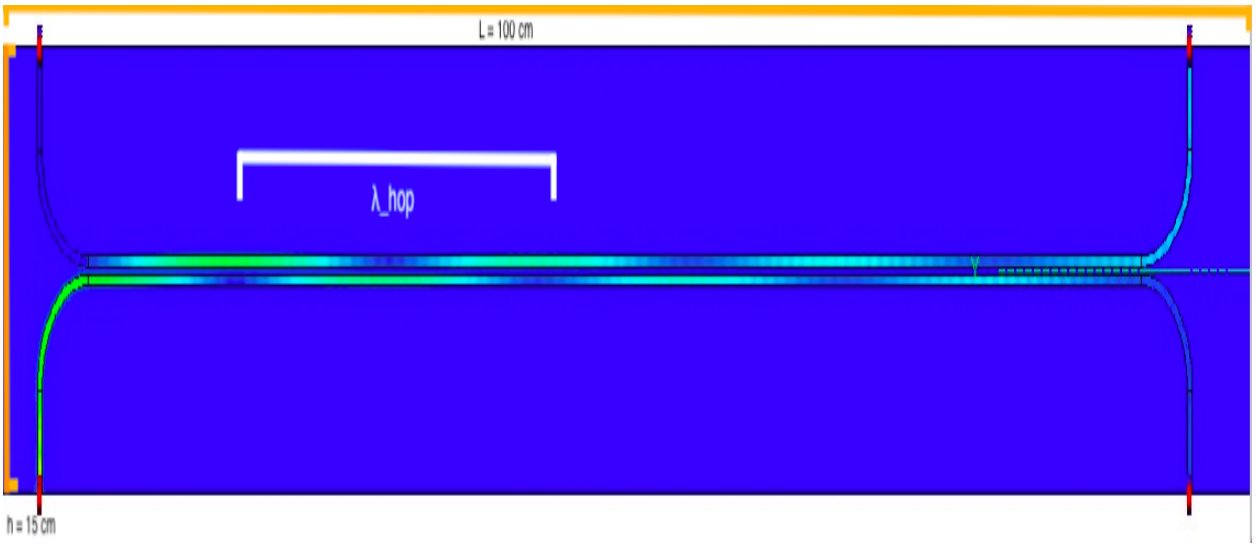

Figure 3.5: FEKO current simulation demonstrating the current "hopping" effect. The current is seen as the highlighted green portion of the trace. Frequency = 9 GHz. The board has a total length of L = 100 cm.

low for effective coupling. After exploring different separation widths, I found that a separation width of 2.5 mm was optimal. However, due to the large size of these simulations, which were almost an order of magnitude greater than my previous simulations, running them in FEKO required several days even with the high performance computing cluster (HPC). Consequently, I relied more heavily on Sonnet than on FEKO.

As we examine the current mapping of the twin microstrip system (see Fig. 3.5), it becomes apparent that the current does not remain in a single trace and instead it hops back and forth as we hoped to observe. This was an exciting moment after months of simulations had built up to this point. After achieving success with the initial simulation at a single frequency, I simulated the system again using a wide range of frequencies, providing us with twenty different simulation results to examine. When analyzing these simulations, we were particularly interested in the total

number of times the current hopped back and forth, as well as the distance between each successive hop λ_{hop}. By "successive hops," I am referring to the distance between two neighboring maxima on the same trace or the distance it takes for the current to hop to one trace and then return to the initial trace. After scrutinizing the data and plotting these two quantities against the frequency, I generated the following two plots (see Fig. 3.6 and Fig. 3.9).

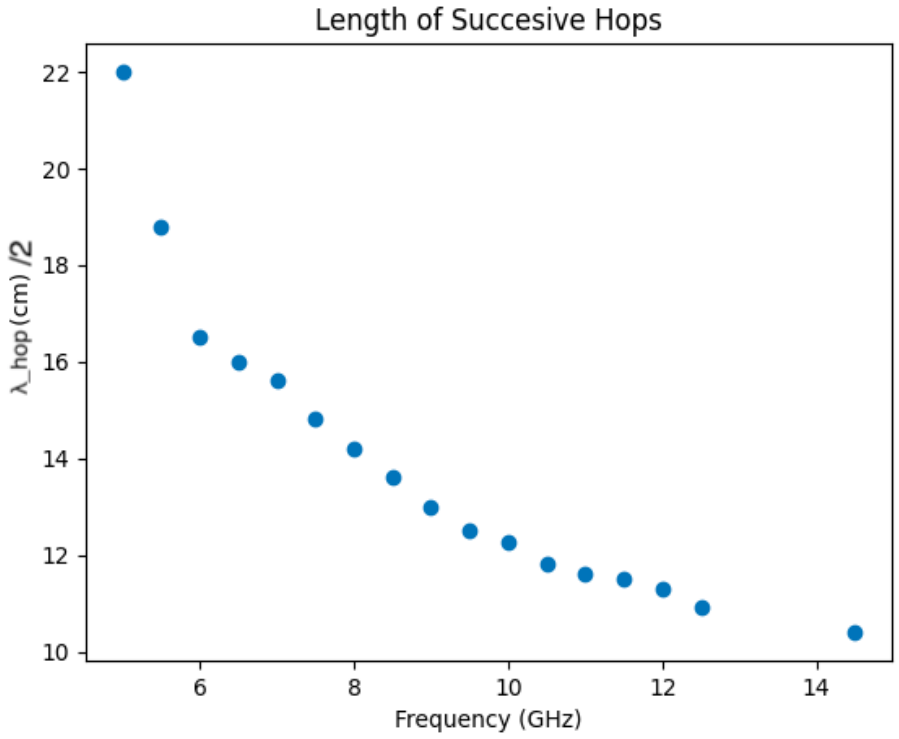

Figure 3.6: A plot of $\frac{\lambda_{hop}}{2}$ vs. the Frequency in GHz compiled from Sonnet simulations.

The graph in Fig. 3.6 shows that the distance between two successive hops decreases monotonically with the frequency.

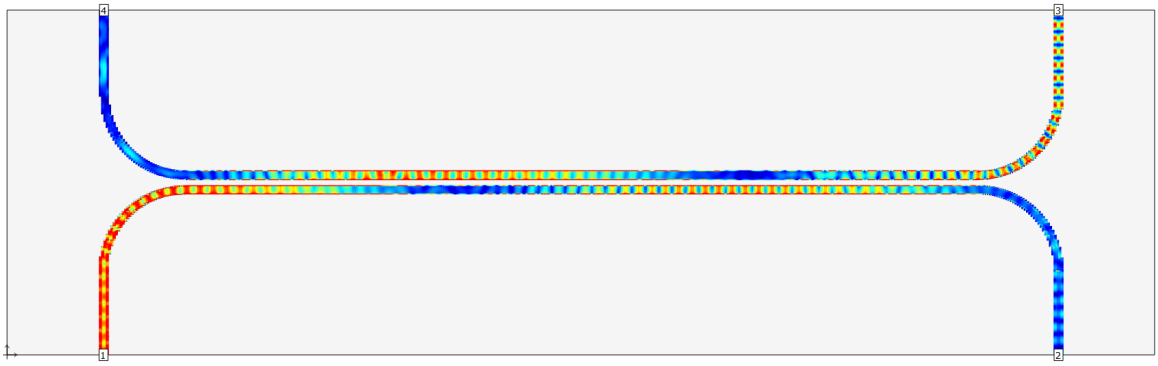

Figure 3.7: Sonnet 9 GHz current simulation results. The length of the board is L = 50 cm.

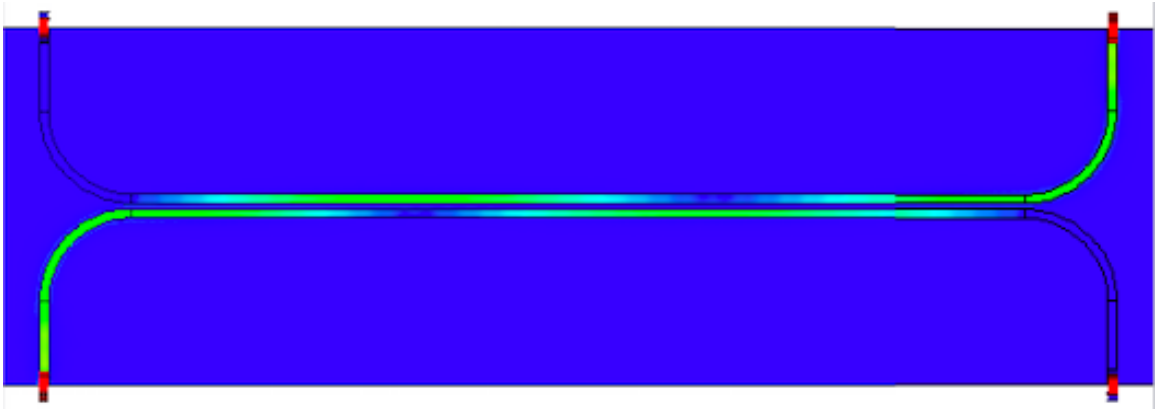

Figure 3.8: FEKO 9 GHz current simulation results.The length of the board is L = 50 cm.

We must also be aware that despite running simulations for identical systems, FEKO and Sonnet do not exactly agree with each other. After conducting the initial Sonnet simulations (see Fig. 3.7), I ran the same system in FEKO at a few select frequencies. While both simulation software demonstrated the desired current hopping effect, interestingly, they disagreed on the number of times the current jumped back and forth between the two traces at higher frequencies. A secondary objective of this project is to evaluate the accuracy of some of the commercial microwave simulation software. Once testing with the physical apparatus commences, we will be able to

verify which of the two software applications is more accurate. Despite their differences, they do agree that the current will hop back and forth. Hence, we felt confident enough to proceed with ordering a RO4350B PCB board with twin microstrip traces.

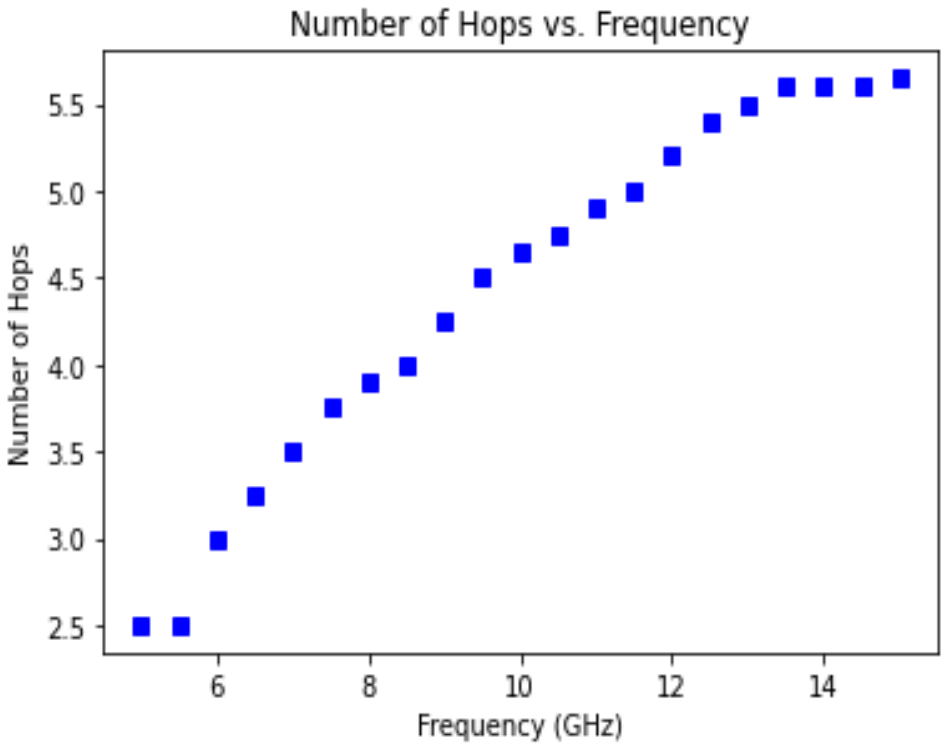

Figure 3.9: A plot of the number of hops vs. frequency created using data from Sonnet simulations.

Examining the plot in Fig. 3.9, we can see that the number of times the current hops from one trace to the other appears to increase roughly linearly with frequency, but eventually plateaus above 13 GHz.

3.7 Twin Microstrip System Final Board Design

Upon conducting several simulations using the originally designed one-meter board, it was revealed that a significant constraint had been overlooked: the PCB manufacturer previously engaged by the laboratory was unable to produce boards of that size. Consequently, the simulations were modified to conform to this revised constraint and were run at the same range of frequencies. As expected, the current hopping effect still occurred, but there were fewer hops due to there being less trace for the current to hop to. After analyzing the results of these simulations, we were satisfied enough to continue and build the board in Eagle, a PCB layout software. However, this software took some time to learn, as it is a very powerful tool with hundreds of features. Since this board required only 1% of the tools that the software offered, we faced a significant hindrance. After the design was made, we immediately sent it off to get a price quote and then ordered them (from EPECTEC.com).

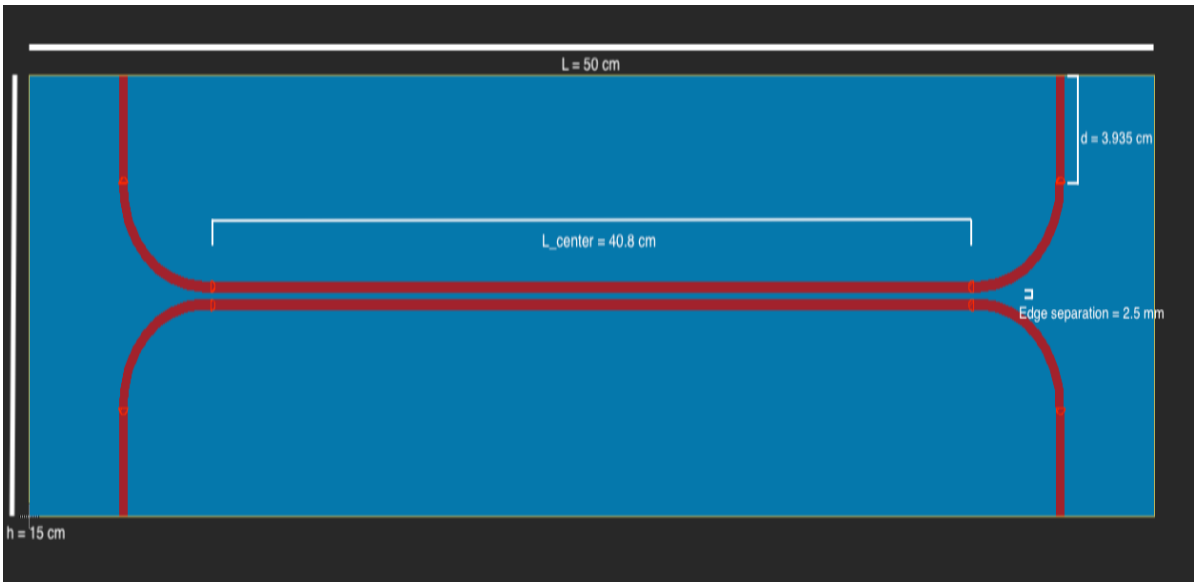

Figure 3.10: Image of the board design in Eagle. Board Specs: trace width = 3.7 mm, PCB Board = RO4350B, board thickness - 1.524 mm = 0.06", turn radius = 35.65 mm

Once the boards had been ordered, we were subject to a lengthy waiting period of 10 business days. While this would not normally be a problem, given that there were only 14 days until the initial thesis was due, and 20 days until my defense, it resulted in a grueling time crunch during the final couple of days.

Chapter 4

Experimental Apparatus

This chapter presents the full process required for taking and analysing data from the physical apparatus. This entails the fabrication of the microwave transmission pickup coil needed to take measurements, using this device to measure a standing wave, and setting up the physical apparatus of the twin microstrip system.

4.1 Fabrication of a Microwave Transmission Pickup Coil

Following Sindu Shanmugadas' work [3], I successfully replicated the fabrication process for a magnetic field sensor. This device is crucial as it allows us to measure the microwave magnetic near field generated by the microwave current in a microstrip trace. The sensor is a tiny mm^2-scale pick-up coil that consists of a microcoaxial cable, whose center conductor forms a small loop with the outer ground sheath conductor. The time varying magnetic flux, $\Phi = \vec{B}_{AC} \cdot \vec{a}$ through the pickup coil loop results in an induced voltage on the coil $\mathcal{E} = -\frac{d\Phi}{dt} = -i\omega\vec{B}_{AC} \cdot \vec{a}$, which can then be detected by a spectrum analyzer (here the "i" indicates a 90· phase shift). Here, $\overrightarrow{B_{ac}} is the microwave magnetic field, and \vec{a}$ is the area of the pickup coil.

The pickup coil is constructed in the following manner (see Appendix A for further details). I utilized a copper coaxial cable with an inner conductor diameter of 0.127

mm and outer conductor diameter of 0.584 mm (Microstock-inc.com part # UT-020). After removing the outer two layers from the end of the cable, I formed the smallest loop possible and soldered it together. Then, I added two layers of heat shrink to reinforce the other end of the device, as the previous models had broken after only a few months of use. The final product minimized the amount of material at the end of the device, to the best of my ability, for improved performance. This is crucial since additional conducting material at the end of the device can negatively affect the measurements being taken. Figures 4.1 and 4.2 show the pick-up coil sensor.

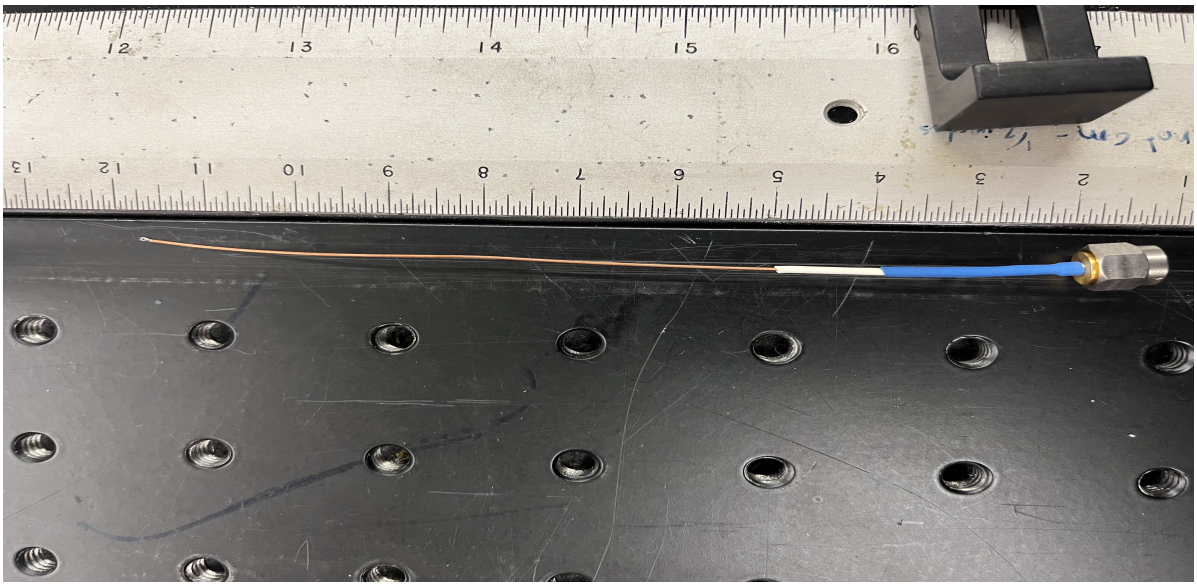

Figure 4.1: An image of the pickup coil placed next to a ruler for scale.

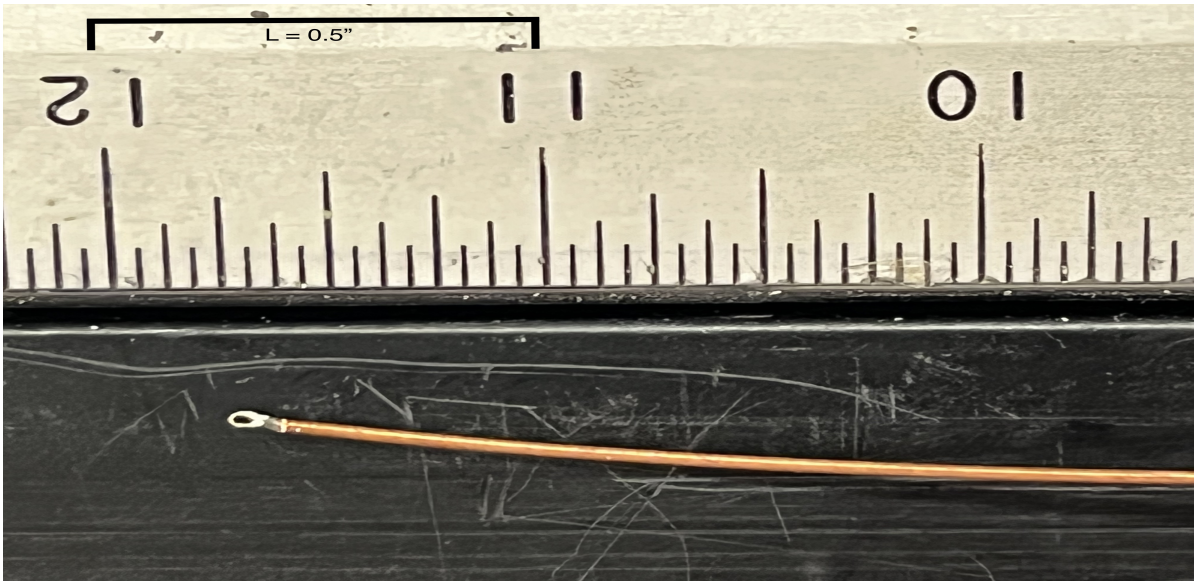

Figure 4.2: A close up image of the loop at the end of the pickup coil.

4.2 Data Collection With Microwave Transmission Pickup Coil

With the newly fabricated microwave transmission line pickup coil, the next logical step is to use it to detect/observe microwave currents in a microstrip transmission line. In a first test, we measured a standing wave generated by a dual output microwave power source, which is used to send counterpropagating microwaves from both ends of a single copper microstrip trace. The power, phase, and frequency of the wave can be controlled by the computer. The microwaves are then passed through a circulator on either end, which has three different ports labeled 1, 2, and 3. If a current is sent into any one of the ports, it will pass along and exit through the next sequential port: 1→2, 2→3, 3→1. As the microwaves travel along the copper trace, when they reach the other end, they will be filtered out by the circulator to prevent them from continuing back into the generator, which could cause damage to it or impede its proper operation.

Once the standing wave is generated along the trace, we can proceed to detect the magnetic component of it with the microwave pickup coil, which is connected to a spectrum analyzer via a coaxial cable. The microwave magnetic near field detected by the pickup coil serves as a proxy for the microwave current in the microstrip trace. Figure 4.3 shows an annotated photo of the setup. There is a sled set up that secures the coil and keeps it as close to the trace as possible, all the while allowing it to be translated along the length of the trace. Using the spectrum analyzer, we can zoom in on the designated frequency and measure the voltage that the coil is picking up. By measuring the pickup coil voltage as a function of position, we can map out a plot of the standing wave that we generated (see Fig. 4.4).

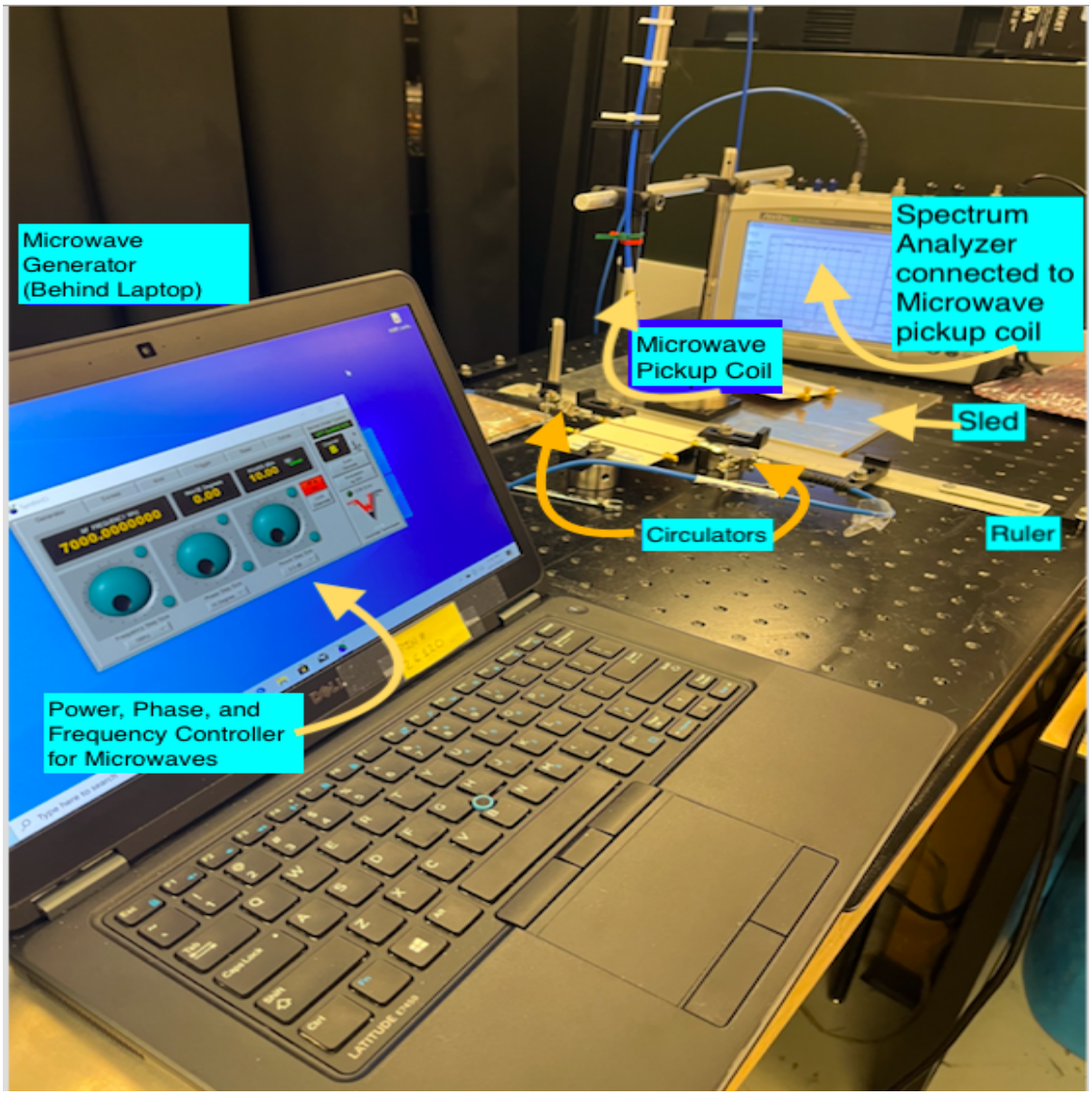

Figure 4.3: Picture of the experimental setup, for measuring a standing wave along a single copper trace.

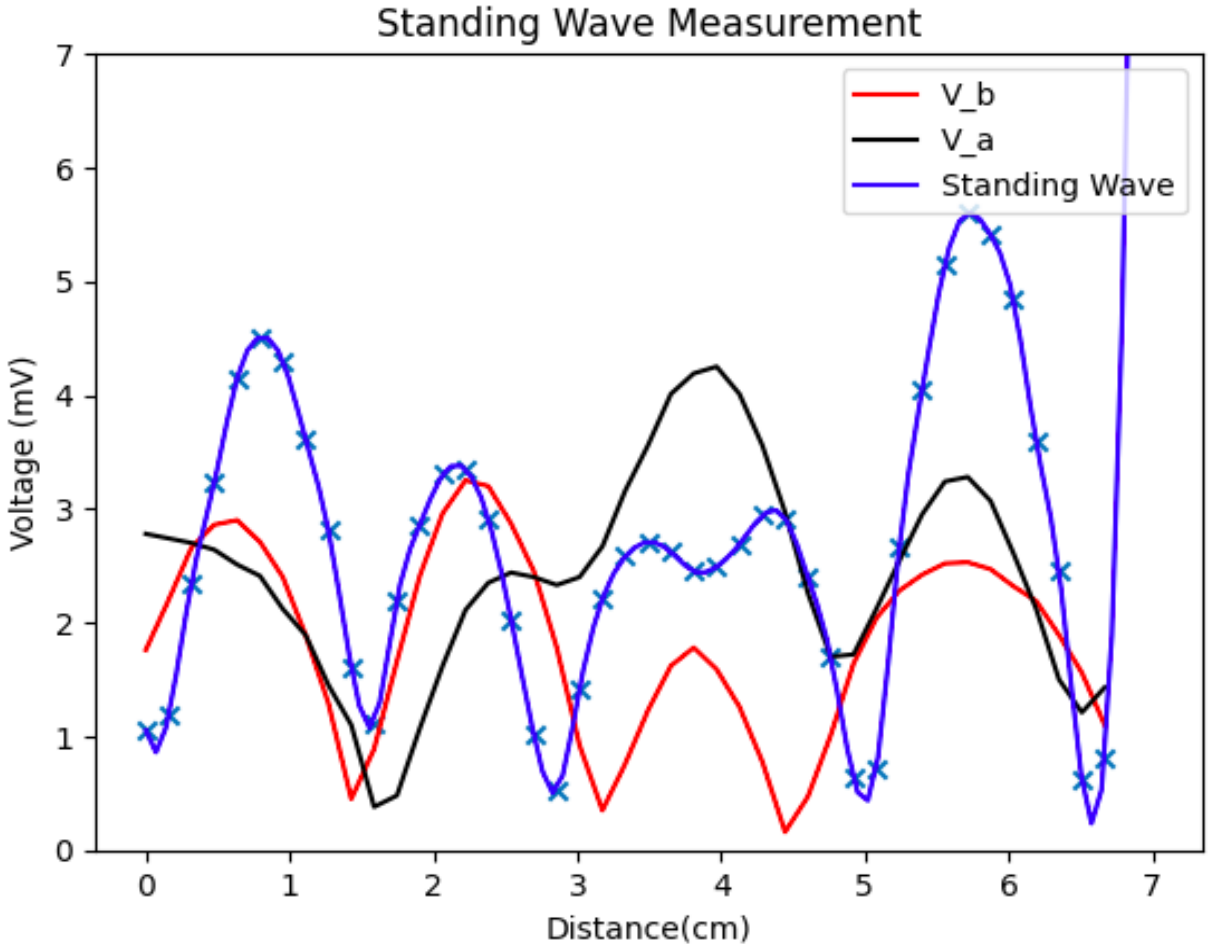

Figure 4.4: Plot of Voltage vs. Distance along trace depicting the shape of a standing wave, at 7 GHz. The standing wave is supported by a 50 Ω microstrip transmission line on a RO4350B microwave PCB board (thickness = 1.524 mm = 0.06") with a trace width of 3.7 mm.

Figure 4.4 shows the results of measuring the 7 GHz standing wave in a microstrip transmission line. First the microwaves directed into either end of the microstrip were separately power balanced (at roughly 10 dBm per output channel). Next, the amplitude of the microwave near field was measured with the pickup coil versus position for each of the microwave sources separately (denoted V_b and V_a in Fig 4.4). Finally, both microwave sources were directed into the microstrip simultaneously to generate the standing wave (blue curve in Fig. 4.4). While the blue curve shows

that a standing wave is present, the V_b and V_a curves show that there is a significant residual standing wave present when there should not be one, i.e. the red and black curves should be flat (probably due to unwanted reflections on the test board).

4.3 Physical Apparatus of Twin Microstrip System

After the long-awaited boards arrived in the mail, research could finally continue. The first task was to measure the trace width to the best of my ability and ensure that it was constant throughout the entire trace, especially the curved sections. After verifying that it was the case to the best of my ability, I learned from William Miyahira how to solder the female SMA connectors onto the end of each trace. Once they were securely attached, I added a 50 Ω termination load to the end of three of these and left the fourth one open to serve as the port to inject the microwave current into (see Fig. 4.5). Professor Aubin and I then adjusted the previous setup to accommodate a board of this size, which was significantly larger than the other ones in use. After attaching the circulator to the remaining port, the new setup was ready for data collection (see Fig. 4.6).

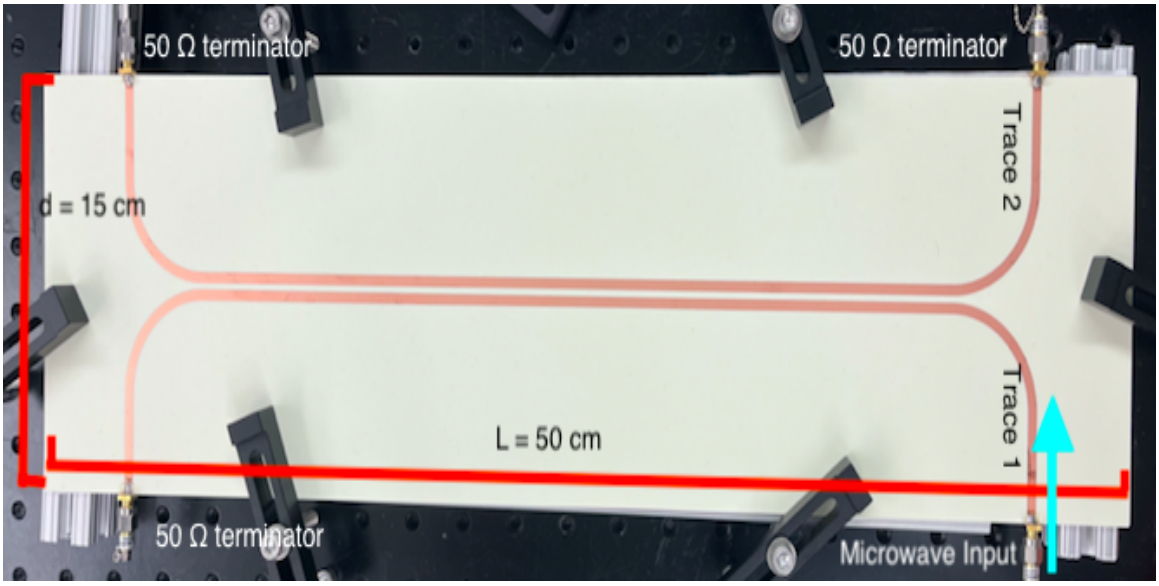

Figure 4.5: An image showing the twin microstrip system apparatus. The microwaves enter the setup on the trace 1 input.

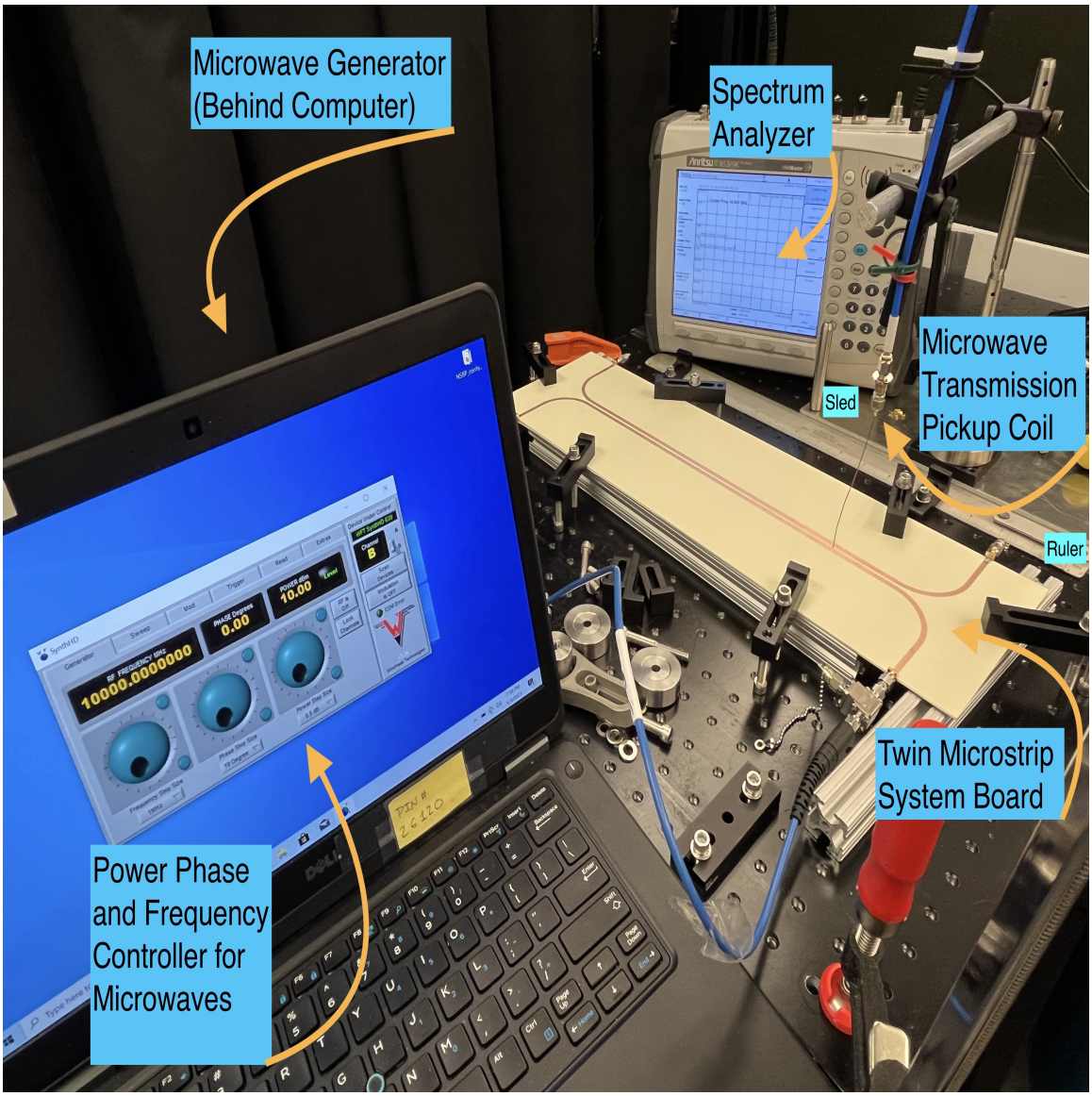

Figure 4.6: Experimental setup for measuring the hopping back-and-forth effect in the twin microstrip system.

Chapter 5

Results

This chapter presents the main experimental results of this thesis. Data collection for this experiment was a time-consuming and arduous process. The pickup coil voltage measured by the spectrum analyzer would change rapidly with the position, so it was imperative to take measurements in very small increments. To ensure the most accurate data possible, I took measurements every $\frac{1}{16}$ of an inch. For a trace that is approximately 40 cm long, this resulted in taking roughly 220 data points from each trace for each round of data collection. Even with a friend helping to speed up the process, it still took around 1.75 hours each time.

5.1 7 GHz Data

With the initial circulator being optimized for the 6.8 GHz frequency, I elected to take data at 7 GHz for my first test. This first dataset provided some interesting results (see Fig. 5.1). When looking at a plot of the data, we are hoping to see that the voltage readings from the two traces are anti-correlated, i.e. when one goes up, the other goes down, which would show that the current has hopped from one trace to the other.

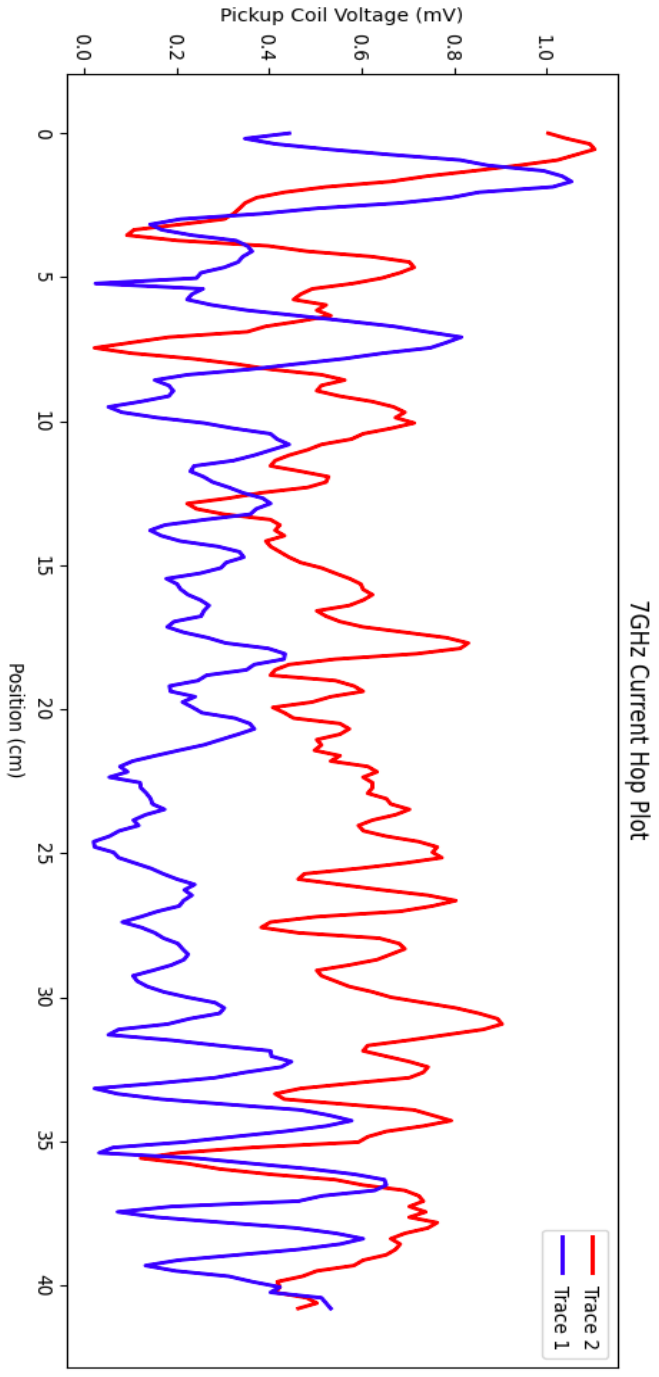

Figure 5.1: A plot of Voltage vs. Distance at the 7 GHz frequency. The microwaves are injected on Trace 1 on the position x=0 side.

Examining the plot in Fig. 5.1, there are a few important features to note. First, the current starts in the trace labeled "Trace 1". Second, we can see a number of small oscillations within the data. In order to try to filter out some of these high frequency variations to observe the long distance trend (i.e. "an envelope" of the data), we can take a running average of the data set (see Appendix B for Python analysis code). This will mean that for each data point we take the 12 entries before it, the 12 entries after it, and average them. We then go through with the next data point and repeat the process until all of the points have been averaged in this way. The plot in Fig. 5.2 shows the result of this running average: the shape of the envelope becomes notably clearer.

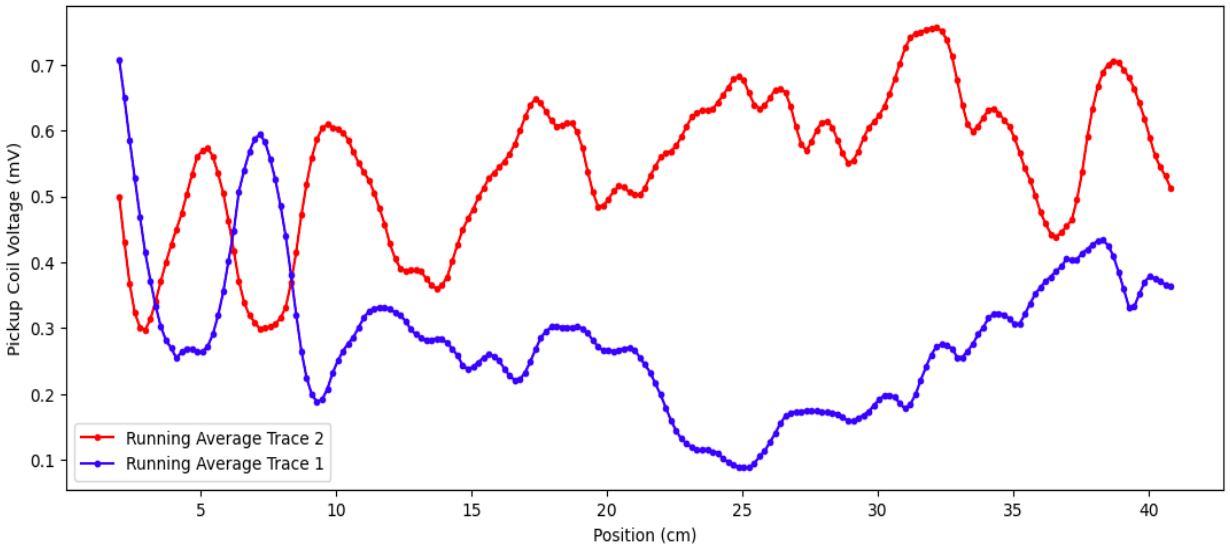

Figure 5.2: A plot of the running average of Voltage vs. Distance at the 7GHz frequency.

Taking a look at the running averages, the current which starts in Trace 1 does certainly appear to hop over to Trace 2, though it does not appear to return. These results provide a possible hint of the anti-correlated data that we are looking for. What this plot fails to do is have the current jump over to one trace and then jump

back. Figure 5.4 shows a Sonnet simulation at 7 GHz, which predicts a hopping distance of $\lambda_{hop} = 40$ cm. This larger hopping distance makes it harder to observe the effect unambiguously. One way we can check the accuracy of this running average plot is to overlay one of the actual data sets and see if the trend line roughly agrees with it.

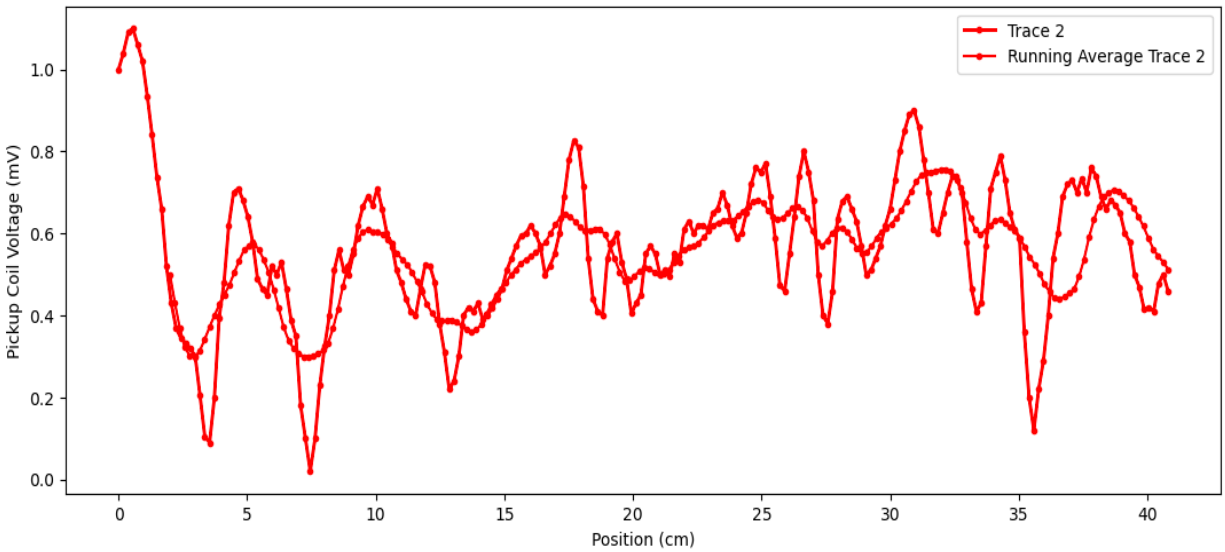

Figure 5.3: A plot of the running average of Voltage vs. Distance at the 7 GHz frequency overlaid with the actual data for Trace 2.

Examining Fig. 5.3, we can see that the running average closely mirrors the raw data. This gives me more confidence in the data and the resulting running average, and the envelope that we see. Next, I moved to a higher frequency in an attempt to see the current hop over, and then hop back.

We previously deduced that the number of times the current jumps is directly correlated to the frequency of the microwaves, so increasing the frequency is one way to hopefully be able to see more hops.

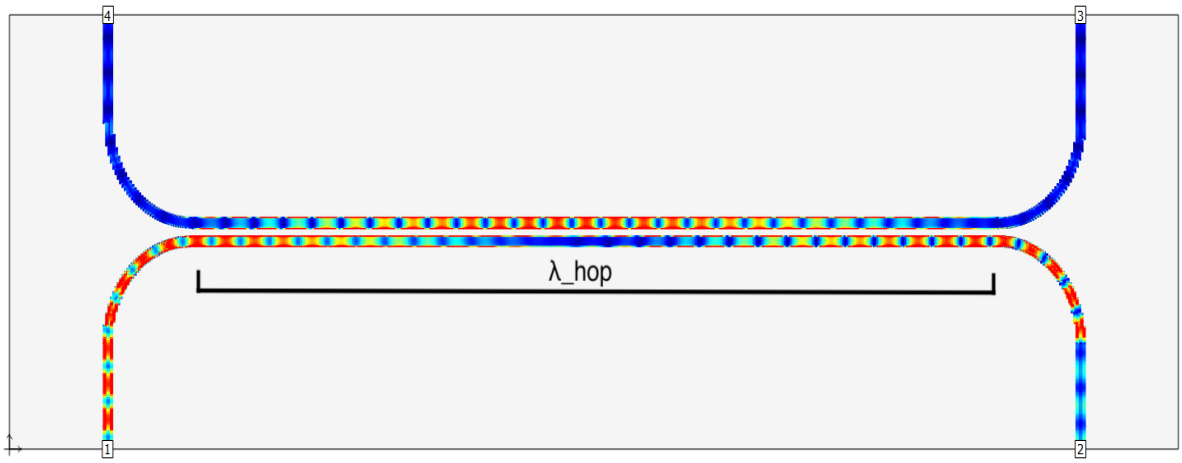

Figure 5.4: An image showing the current mapping for a Sonnet simulation of the twin microstrip system running at 7 GHz. This simulation predicts $\lambda_{hop} = 40$ cm.

5.2 14 GHz Data

Data collection at the 14 GHz frequency involved the exact same process as 7 GHz. In both rounds of data collection, the signal on the spectrum analyzer tended to oscillate between a range of values. When choosing which value to record I would write down the value that I deemed to be the average of the range I was seeing. After collecting another 220 data points per trace, I obtained the data plotted in Fig. 5.5.

In this round of data collection, the current started in Trace 1. The plot shows that between x=10 cm and x=25 cm the current has hopped over to trace 2. However, after x=25 cm, there is roughly equal current in both traces. Turning to the data analysis techniques we used for 7 GHz, we can get a better picture of whats going on.

Looking at the running averages for the 14 GHz results (see Fig. 5.6 and Fig. 5.7) confirms what I initially deduced. The current starts in Trace 1, largely moves to Trace 2 between x = 10 cm and x = 25 cm, and then exists relatively equally in

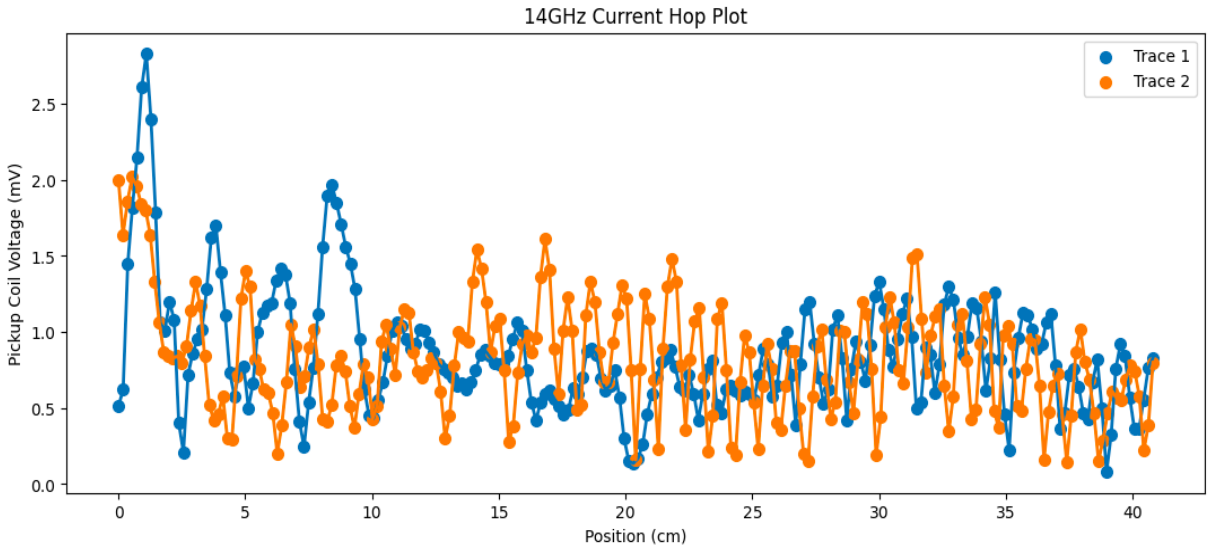

Figure 5.5: A plot of Voltage vs. Distance at the 14 GHz frequency. The microwaves are inserted on trace 1 on the x=0 position side.

the two traces for x $\geq$ 25 cm. My best guess for this behavior is that in the last $\frac{3}{8}$ of the two traces, since the current never fully left either of the two traces, it managed to reach a point of relative equilibrium between the two when it attempted to jump back to the Trace 1.

At 14 GHz, the range of values that the voltage jumps between when measuring here is notably larger than the range at 7 GHz. Because of this, it is my belief that at higher frequencies it is essential to take even more data points in order to ensure the data is as accurate as possible. To ensure our analysis is sound, I have once again plotted the data with the raw data overlayed onto the plot of running averages.

Comparing the collected data to the simulations (Fig 5.7, 5.8, 5.9, 5.10), we can see that the simulation suggests λ_{hop} is 22 cm, whereas the collected data displays it being around $\lambda_{hop} = 30$ cm.

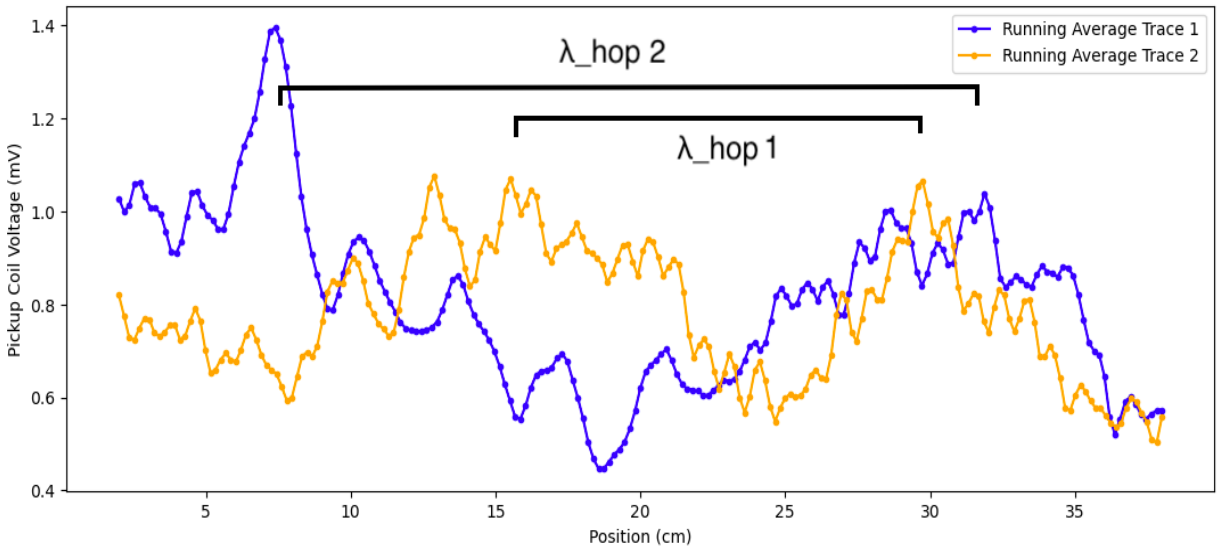

Figure 5.6: A plot of the running average of Pickup Coil Voltage vs. Distance at the 14 GHz frequency. This plot indicates $\lambda_{hop} = 28$ cm or $\lambda_{hop} = 15$ cm.

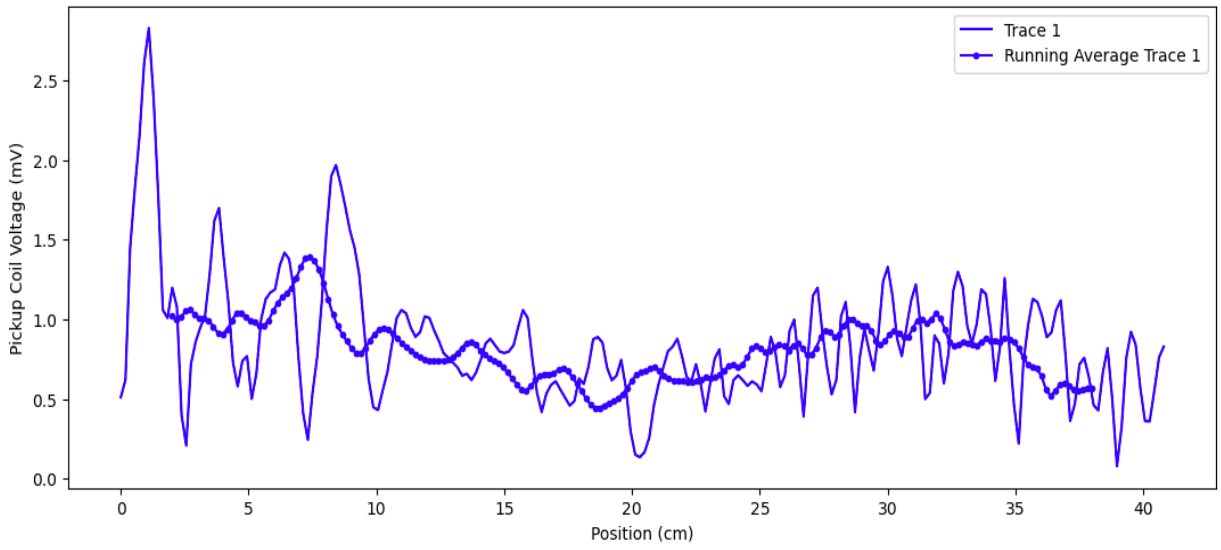

Figure 5.7: A plot of the running average of Pickup Coil Voltage vs. Distance at the 14 GHz frequency overlaid with the actual data for Trace 1.

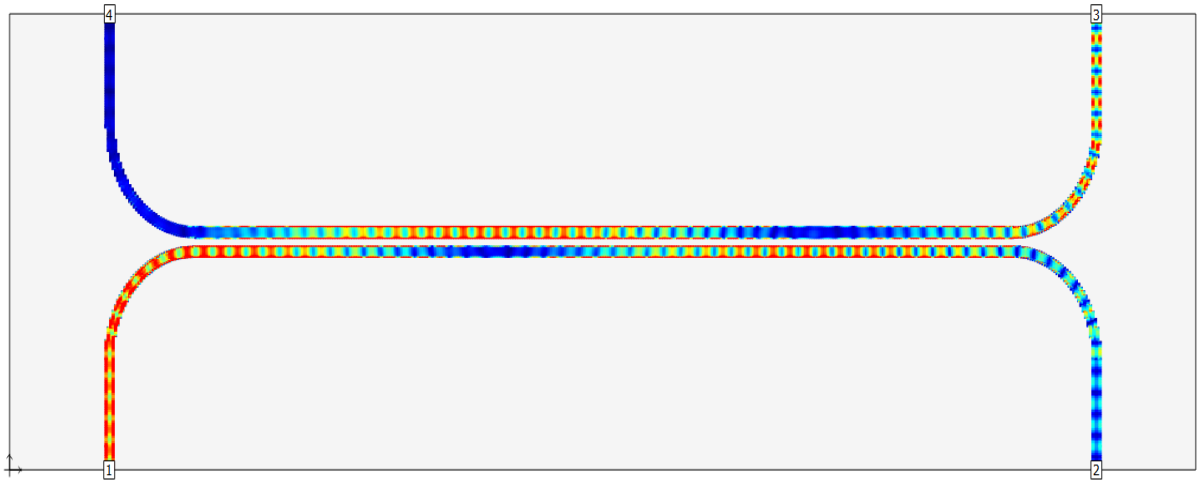

Figure 5.8: An image showing the current mapping for a Sonnet simulation of the twin microstrip system running at 12 GHz.

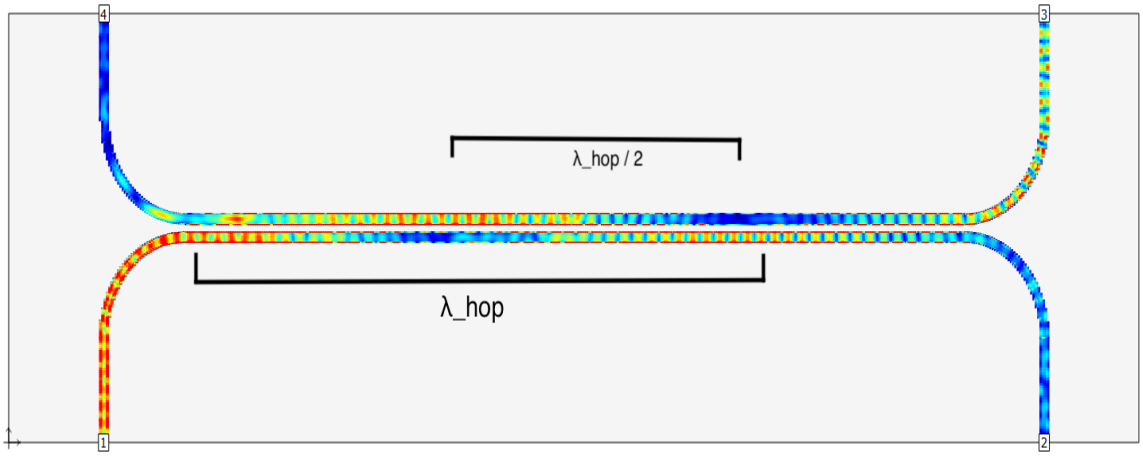

Figure 5.9: An image showing the current mapping for a Sonnet simulation of the twin microstrip system running at 14 GHz. This simulation predicts $\lambda_{hop} = 30$ cm.

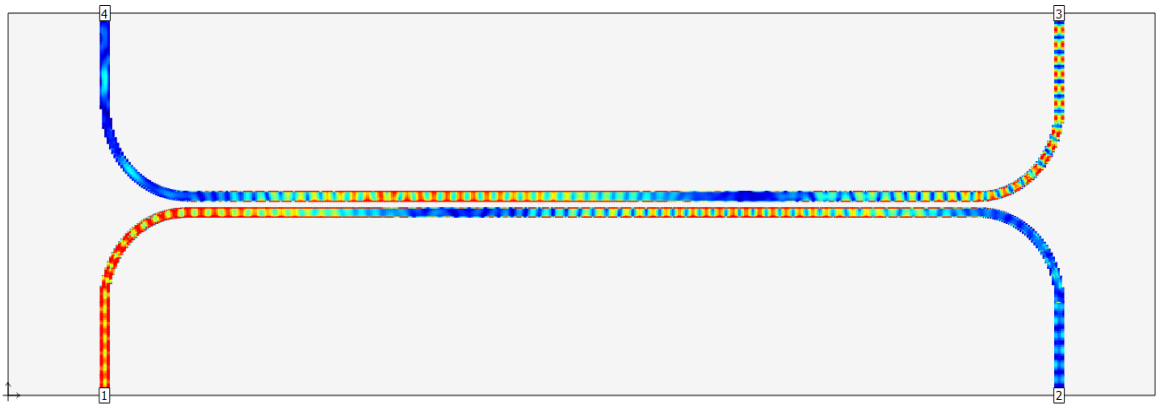

Figure 5.10: An image showing the current mapping for a Sonnet simulation of the twin microstrip system running at 14.5 GHz.

As we can see in Fig. 5.6, the running average is a good representation of the raw data. Comparing that data to Fig. 5.9, we can see that the simulation (Sonnet) and actual data give comparable values for λ_{hop}.

Chapter 6

Conclusion/Outlook

Although I did not observe the current hopping back and forth between the two traces perfectly clearly, I am confident that I did observe the desired effect. The 14 GHz frequency provides more compelling data than the 7 GHz frequency, but even at 7 GHz the effect is visible to some extent. Given more time to collect and analyze data, more supporting measurements could be made.

Moving forward, whoever undertakes this project will have all the necessary tools to study and analyze the effect, but they will need to commit a sufficient amount of time to data collection. Looking forward, here are a few possible avenues for future work:

- Collecting and analyzing data at 10 GHz to shed light on the accuracy of the Sonnet and FEKO simulations since we have simulation data from both at that frequency which disagree with each other.
- The analysis of higher frequencies could be done using the new spectrum analyzer (Agilent E4407B, 26.5 GHz).
- Attaching another microwave signal to the opposing trace to attempt to measure the eigenstates of the system by controlling the phase of the two inputs.
- Finding a way to automate or speed up the data collection process would greatly

benefit the project. It could possiblybe achieved through the use of a Raspberry Pi or another microcontroller to control the data collection process and minimize human error.

Appendix A

Fabrication of Microwave Transmission Pickup Coil

1. The first step after acquiring the coaxial cable is to remove the layer of copper on the outside. It is important to note that we only need to remove around a centimeter of the copper from the end of the cable. To do this, I first laid the end of the cable flat against a solid surface. I then took a new razor blade and started with it perpendicular to the cable. I gently applied some force downward, and performed a scooping motion with the blade. The purpose of this is to try and get through the copper layer without cutting through of the other layers of the cable. It will take some time to make an initial incision into the copper. After repeating this step a number of times, either a flake of the copper will come off, or the copper will stay stuck together and the entire sheath of it will come off.

2. After removing the copper layer, we can see that there are two more layers, a teflon layer, and the inner conductor. The teflon is extremely easy to remove. I found that what works best is taking the razor blade and gently cutting straight downward on the newly exposed teflon. Then rotating the coaxial cable until you have made an incision all around the teflon layer. At this point it can easily

be slid off gently leaving the inner conductor.

Figure A.1: Exposed teflon layer after the removal of the copper layer.

=

3. Once all of the Teflon has been removed, we are left with the thin inner conductor which is essentially just a wire at this point. This is the most fragile piece so it is important to not bend it too violently when manipulating it's shape. The goal here is to make the smallest loop we possibly can with our newly exposed wire. A fellow student Adi de la Guardia suggested the idea of using the lead

from a mechanical pencil to wind the loop around. This makes it incredibly simple to form the loop, and since there will likely be some excess wire after making the loop, I usually trim most of it away.

Figure A.2: The loop formed from the inner conductor layer.

4. Once the loop has been formed, the last step is to deposit a glob of solder onto the end of our loop, firmly attaching it to the copper section of the cable. I found that what worked best for me was depositing a tiny glob of solder onto the tip of the soldering iron, and then wiping that glob onto the designated place. We want to minimize the size of the glob of solder so that we have as little matter as possible near the loop. After the cable cools down it is finished.

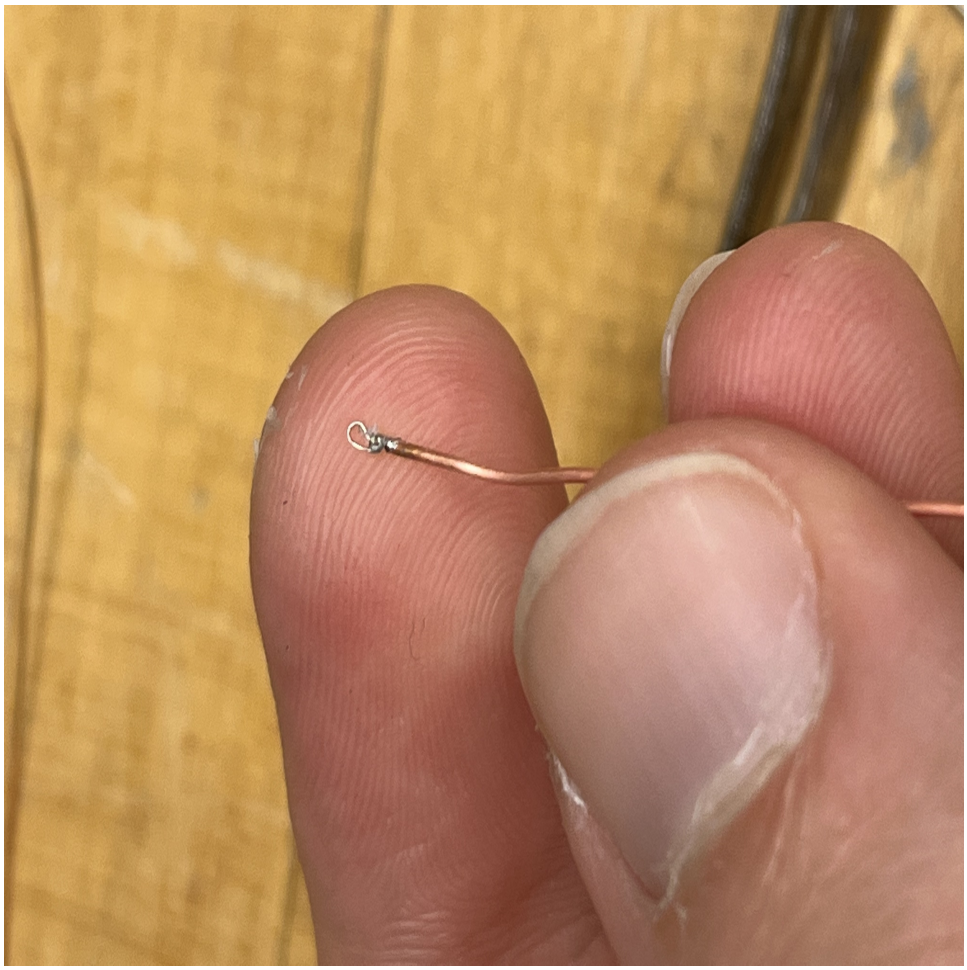

Figure A.3: Completed loop soldered together.

Extra Notes

At the other end of the coaxial cable, because it is so thin it is very easy for it to get worn down over time and break. In order to fortify it I attempted to deposit a thick glob of solder at this end, but was somewhat unsuccessful in having it taper off elegantly. Heat shrink works much better. I applied two layers of heat shrink with varying degrees of thickness to drastically increase the durability of the pickup coil.

Appendix B

Code sample

The following is the Python code which will calculate the running averages of the collected data from each trace.

```
/************************************************************/

import numpy as np
import matplotlib.pyplot as plt
x11 = np.linspace(0, 40.8, 224)
x1 = np.linspace(2, 38, 201)
x2 = np.linspace(2, 38, 206)
y1= [0.512,0.621,1.45,1.82,2.15,2.61,2.83,2.4,1.79,1.06,...]
y2= [2, 1.64, 1.86, 2.02, 1.96, 1.84, 1.80, 1.64, 1.33, 1.06, 0.864, ...]
plt.figure(figsize=(13, 5))

window_size = 12
running_average1 = np.convolve(y1[12:], np.ones(window_size)/window_size, mode='valid')
running_average2 = np.convolve(y2[12:], np.ones(window_size)/window_size, mode='valid')

# Plot the original data and the running average

#ax.plot(data, label='Original data')
plt.plot(x11, y1,'g' ,label='Trace 1')
plt.plot(x1, running_average1, 'g.-',label='Running Average Trace 1')
plt.plot(x2, running_average2, 'b.-',label='Running Average Trace 2')
plt.legend()
plt.show()
```

Appendix C

Making Curves in Eagle

Making curves in Eagle is not as difficult as it may initially seem. Similar to FEKO, we first must make the two horizontal traces we wish to connect with a curve. Once that has been done, we will select the line tool. With this tool we can then specify the thickness of the line we would like to draw, so we will set this to the same thickness as the trace itself. Then at the top of the screen we can specify the type of line we would like to draw. We will select the curved option at the bottom. Then, starting at one trace and going to the other we can draw a line, and eagle will curve it properly for us!

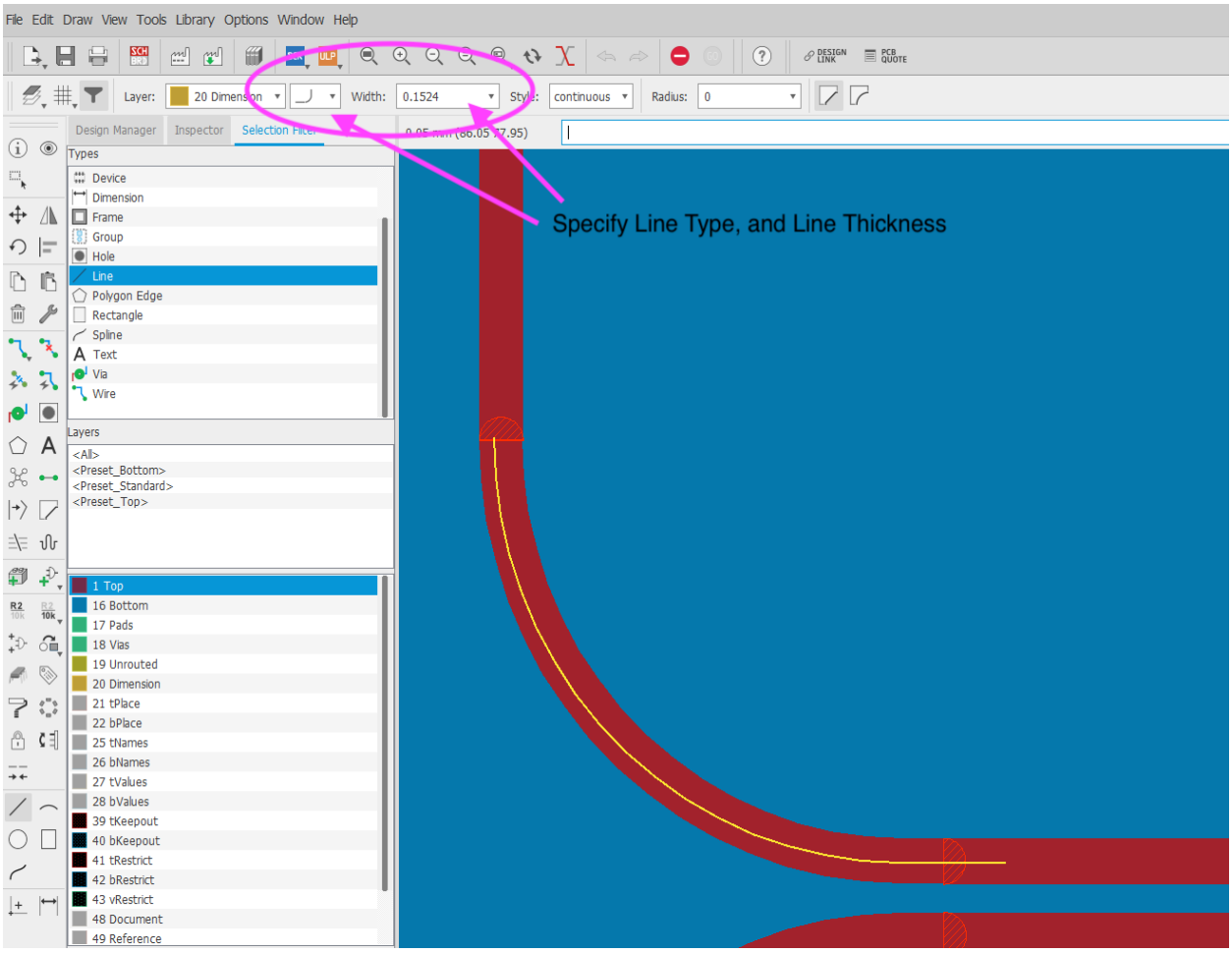

Figure C.1: An image showing the eagle display.

Bibliography

[1] [Miyahira et al.] W. Miyahira, A. P. Rotunno, D. Do, and S. Aubin, "Microwave atom chip design", MDPI Atoms 9, 54 (2021).

[2] Shuangli Du, Ph.D. thesis, 2021. AC and DC Zeeman interferometric sensing with ultracold trapped atoms on a chip.

[3] Sindu Shanmugadas, senior thesis, December 2021. Measuring the Magnetic and Electric Fields of a Microwave Lattice for Atom Chip Development

[4] Properties of Current Hopping in Microwave Traces, A Beginning Study through Simulation. Sindu Shanmugadas Summer 2020 Research at William & Mary's Ultra-Cold AMO Lab, Seth Aubin